universität wien

MASTERARBEIT / MASTER'S THESIS

Titel der Masterarbeit / Title of the Master's Thesis

„The role of the transcription factor Aiolos in marginal zone B cell development“

verfasst von / submitted by

Alexander Athanasiadis, BSc

angestrebter akademischer Grad / in partial fulfilment of the requirements for the degree of

Master of Science (MSc)

Wien, 2021 / Vienna, 2021

Studienkennzahl lt. Studienblatt / degree programme code as it appears on the student record sheet:	UA 066 834
Studienrichtung lt. Studienblatt / degree programme as it appears on the student record sheet:	Masterstudium Molekulare Biologie
Betreut von / Supervisor:	Meinrad Busslinger PhD

Acknowledgements:

I want to thank my supervisor Meinrad Busslinger for the opportunity to do my master's thesis in his lab. I want to also thank him for all the time and support that helped shape this thesis.

Furthermore, I want to especially thank Tanja Schwickert, for her exceptional help, support and for introducing me to the project and helping with the planning of experiments and interpretation of results.

I am grateful for my colleagues in the Busslinger lab that helped and created a nice working environment, also considering the difficult times during a global pandemic. Thank you for all the laughs.

Finally, I want to thank my family and friends for always being there for me.

Without your help, this thesis would not have been possible.

Thank you.

Zusammenfassung:

Marginal zonen (MZ) B-Zellen befinden sich in der Milz von Mäusen, wo sie eine entscheidende Rolle im adaptiven Immunsystem spielen. Sie helfen, die Zeit bis zur vollständigen Aktivierung des adaptiven Immunsystems zu überbrücken, indem sie polyreaktive Antikörper von niedrigerer Affinität produzieren als es follikuläre (FO) B-Zellen nach durchlaufener Keimbahnreaktion tun. MZ B und FO B-Zellen entstehen aus denselben Vorläufer-Zellen im Knochenmark, aber wo genau sich die Zelllinien aufteilen, um diese unterschiedlichen Funktionen zu erfüllen, ist noch nicht restlos geklärt.

Der Transkriptionsfaktor Aiolos (Ikzf3), der Teil der Ikaros Familie der Zink Finger Transkriptionsfaktoren ist, spielt eine wichtige Rolle in der Entstehung von MZ B-Zellen, da *Ikzf3* Knock-Out (KO) Mäuse keine MZ B-Zellen mehr haben, während FO B-Zellen vorhanden sind. Wie genau Aiolos die Entwicklung von MZ B-Zellen beeinflusst ist unbekannt, auch da lediglich keimbahn-deletierte KO Mäuse für bisherige Studien verwendet wurden. Hier zeigen wir erstmals mittels konditioneller Geninaktivierung in *Ikzf3*$^{fl/fl}$*Cd23*-Cre Mäusen, dass der Verlust an MZ B-Zellen ein B-Zell intrinsischer Phänotyp ist. Wir zeigen, dass Aiolos deletierte B-Zellen eine erhöhte B-Zell Rezeptor Aktivität haben, was zu veränderter mTORC1 Signalübertragung führt. Der Verlust von Aiolos kann durch ektopische Überexpression von Notch1 gerettet werden. Mittels mRNA-Seq in diesen geretteten MZ B-Zellen sowie Aiolos-ChIP-Seq in Wildtyp Mäusen analysiere ich Aiolos-regulierte Gene.

Abstract:

Marginal Zone (MZ) B cells reside in the spleen of mice and are an essential part of the adaptive immune system. They produce polyreactive antibodies of lower affinity and thus help to bride the temporal gap until a full adaptive immune response by follicular (FO) B cells undergoing the germinal center reaction can be mounted, leading to the production of high affinity antibodies. MZ and FO B cells arise from the same progenitors in the bone marrow, but where exactly the lineag split takes place and gives rise to these different functions is still not fully understood.

The transcription factor Aiolos (Ikzf3), which is part of the Ikaros family of zink finger transcription factors, has been shown to play an important role in MZ B cell development, as Aiolos knock-out (KO) mice lack MZ B cells while FO B cells are still present. However, it is not completely understood how Aiolos influences MZ B cell development as most studies used germline deleted Aiolos KO mouse models for their research. Here we show for the first time with conditional mutagenesis, that the loss of Aiolos-deficient MZ B cells is B-cell-intrinsic. We show that Aiolos-deficient B cells have higher B cell receptor signaling which results in differences in mTORC1 signaling. The loss of Aiolos can be rescued by overexpressing the intracellular domain of Notch1. I performed mRNA-Seq with these rescued MZ B cells and Aiolos-ChIP-Seq in wildtype mice to identify genes regulated by Aiolos.

Inhaltsverzeichnis

ACKNOWLEDGEMENTS: 2

ZUSAMMENFASSUNG: 3

ABSTRACT: 4

1. INTRODUCTION: 7

1.1 B CELL DEVELOPMENT 7
1.1.1 B CELL DEVELOPMENT DURING EMBRYOGENESIS 7
1.1.2 EARLY DEVELOPMENT IN THE BONE MARROW 7
1.1.3 DEVELOPMENT IN THE SPLEEN 9
1.2 MARGINAL ZONE B CELLS 9
1.2.1 GENERAL DIFFERENCES BETWEEN MZ AND FO B CELLS 9
1.2.2 POSITIONING OF MZ B CELLS IN THE MARGINAL ZONE REQUIRES MULTIPLE SIGNALS 10
1.3 FACTORS INVOLVED IN MZ B CELL DEVELOPMENT 11
1.3.1 BCR SIGNALING INTENSITY 11
1.3.2 NF-KB SIGNALING 11
1.3.3 MICRORNA MIR146A 13
1.3.4 NOTCH2 SIGNALING AND ADAM10 PROTEASE 13
1.3.5 THE TRANSCRIPTION FACTOR AIOLOS (IKZF3) 14
1.3.6 AIM OF THIS STUDY 15

2 RESULTS: 17

2.1 CHARACTERIZATION OF CD23-CRE MOUSE LINE 17
2.2 *IKZF3*$^{-/-}$ MICE LACK MZ B CELLS 17
2.3 *IKZF3*$^{-/-}$ MICE SHOW INCREASED CLASS SWITCHING IN VITRO 22
2.4 CHIP-SEQ AND MRNA-SEQ IN CONTROL AND AIOLOS-DEFICIENT B CELLS 22
..... 29
2.5 *AIOLOS*-DEFICIENT B CELLS HAVE DEREGULATED CD23 AND CD21 EXPRESSION 29
2.6 AIOLOS-DEFICIENT B CELLS HAVE STRONGER BCR SIGNALING 31
..... 32
2.7 AIOLOS KO MICE HAVE HIGHER P-S6 LEVELS 33
..... 36
..... 37
2.8 RAPAMYCIN TREATMENT DOES NOT RESCUE AIOLOS-DEFICIENT MZ B CELLS 37
2.9 PTEN KO CAN RESCUE MZ B CELLS 38

3 DISCUSSION: 41

4 MATERIALS AND METHODS: 44

4.1 GENERATION OF AIOLOS KO MICE 44
4.2 FLOW CYTOMETRY 44
4.3 DEFINITION OF POPULATIONS IN FLOW CYTOMETRY 45
4.4 B CELL PURIFICATION 46

4.5 HISTOLOGY **46**
4.6 CA^{2+} FLUX - BCR SIGNALING **46**
4.7 ANALYSIS OF PROTEIN PHOSPHORYLATION LEVELS BY FLOW CYTOMETRY **47**
4.8 RAPAMYCIN TREATMENT **48**
4.9 IN VITRO STIMULATION FOR CSR **49**
4.10 CHIP-SEQ **49**
4.11 MRNA-SEQ **51**

6 REFERENCES: **53**

1. Introduction:

1.1 B cell development

B cells are part of the adaptive immune system, where they provide protection against a virtually unlimited number of pathogens by production of antibodies. Defects in B cell immunity and development have major complications like autoimmunity or malignancy.[1] The B cell population consists of multiple subsets and cell types, which have different functions. These subsets arise during development by a multitude of different signals and transcription factors that help to shape these cell-fate decisions.

1.1.1 B cell development during embryogenesis

Where the first progenitor cells of the hematopoietic system develop during early embryogenesis is not yet fully understood. The earliest cells seem to arise from the placenta, yolk sac and the aorta-gonad-mesonephros, which then give rise to the fetal liver.[2] After the fetal liver expands, hematopoietic stem cells (HSC) then colonize the embryonal bone marrow (BM), spleen and thymus. In adult mice, the only source of B cells is the BM. Cells from there then colonize the spleen and thymus.[2]

1.1.2 Early development in the bone marrow

Pro-B cells: The early stages of B cell development in the BM are centered around recombination events of the immunoglobulin gene segments, which ultimately lead to the production of a functional B cell receptor (BCR). Common lymphoid progenitor cells (CLP) in the BM give rise to so-called pro-B cells. These are expressing recombination-activating genes 1 and 2 (Rag1, Rag2; cellectively termed Rag here), which initiate Immunoglobulin heavy (IgH)-chain rearrangement which leads to a diverse antibody repertoire. The H-chain locus consists of many different variable (V_H), diversity (D_H) and joining (J_H) gene segments. These are rearranged in two steps: first, one D_H and one J_H are joined to form DJ_H, followed by a second step joining one V_H to DJ_H forming a finished VDJ segment.[3]

The order of recombination is in part regulated by epigenetic marks. For example, the J_H segments are high in the histone modification H3K4me3, which is bound by Rag2, causing these segments to be rearranged first.[4] Other studies showed that, especially in pro-B cells, the physical distance in the nucleus from D_H to both distal and proximal V_H segments was similar, allowing for a more homogenous recombination frequency, irrespective of distance on the genome.[5]

By "randomly" selecting one V_H, D_H and J_H segment from the entire available pool, a high amount of diversity in BCR's arises between B cells. Further diversification arises through the random addition of so called *new* (N) or *palindromic* (P) nucleotides between the joined segments during recombination as well as through processing by certain nucleases.[6] Ultimately, this *randomness* is the reason, why every B cell expresses a unique BCR.[7] After recombining, the VDJ segment is expressed with the constant chain μ (Cμ) on the surface of the cell. There it interacts with the surrogate light chain (SLC) components Lambda5 (λ5) and Vpre-B to form a pre-BCR. The cell is now a large pre-B cell.[8]

Large pre-B cells: Large pre-B cells start proliferating, which is triggered by antigen independent signaling through the pre-BCR and leads to an increase in total B cell numbers. Pre B cells also temporarily stop expressing Rag.[8]

Small pre-B cells: The next stage during development is the small pre-B cell stage, which is characterized by downregulation of SLC components and re-expression of Rag for the recombination events in the immunoglobulin light (IgL) chain. There are two possible L-chain loci, κ or λ, that can be rearranged and each provide multiple different downstream C_L regions. In C57BL/6J mice, the κ light chain locus consists of around 101 V genes, 4 J genes and a single C gene. The λ light chain locus consists of just 3 V genes that can be joined to one of two J-C pairs. Multiple subsequent rearrangement steps in the light chain loci can happen, if self-reactive BCR's are formed. For example, the κ locus on the first chromosome can undergo recombination and the resulting light chain associates with the heavy chain to form a complete BCR. If this receptor is autoreactive, the cell can undergo a secondary rearrangement of the κ locus on the same chromosome. If the resulting BCR still is autoreactive, further rearrangements steps of the λ loci can happen on the first and then the second chromosome. [9,10] If after multiple rearrangements still no self-tolerant BCR is formed, the cell will undergo apoptosis. Only if the BCR is not autoreactive and experiences tonic signaling, the cell is positively selected and now termed a immature B cell.

Immature B cells: Immature B cells express the membrane form of IgM that, together with CD79A (Igα) and CD79B (Igβ), form the BCR complex. Immature B cells are especially sensitive to apoptosis but also lose the ability to further edit their BCR.[7] They then leave the BM and further mature in the spleen, where they are termed "transitional" B cells.

1.1.3 Development in the spleen

Transitional B cells: Two distinct subsets of transitional B cells are characterized in the spleen. Transitional 1 (T1) which then give rise to transitional 2 (T2) B cells. In humans, T1 cells have been shown to be very susceptible to spontaneous apoptosis as a form of negative selection. T2 cells on the other hand start becoming more responsive to antigen stimulation for positive selection.[11] T1 and T2 cells can be distinguished by the surface expression of CD21 and CD23 where T1 cells are $CD21^{-}CD23^{-}$ and T2 cells are $CD21^{+}CD23^{+}$.

Mature: After the T2 stage the cells ultimately become naïve mature and reside either in the follicle or the marginal zone of the spleen and are termed follicular (FO) B cells or marginal zone (MZ) B cells, respectively. Where exactly the cell fate decision between FO and MZ B cells takes place is still not fully understood.

1.2 Marginal Zone B cells

1.2.1 General differences between MZ and FO B cells

The marginal zone lies at the boundary of the red and white pulp of the spleen and MZ B cells therefore can sample the blood for pathogens.[12] In contrast, naïve mature FO B cells reside in the follicles of the spleen but also constantly recirculate through the BM, blood, lymph, lymph nodes and Peyer's patches. They interact with T helper cells to produce high affinity antibodies in the so-called germinal center (GC) reaction.[13]

MZ B cells play various roles during immunity. They are considered to be of an "innate" like phenotype, meaning that they can differentiate into short-lived plasma cells and constitute a first line of defense against invading pathogens.[14] Unlike FO B cells, MZ B cells can express polyreactive BCR's. These can recognize a broader range of pathogens through microbial patterns and rapidly produce antibodies of lower affinity and neutralizing potential compared to FO B cells. This helps to bridge the time gap until a full adaptive response involving FO B cells can be mounted.[14]

MZ B cells can respond to T-cell-dependent antigens as well as T-cell-independent antigens. They have been shown to express high levels of Toll Like Receptor 4 (TLR4) that reacts to LPS, allowing for a strong T-independent response triggered directly by pathogens.[13]

MZ B cells also participate in T-dependent immunity by capturing systemic antigens followed by shuttling to the follicle and dumping the antigens on follicular dentritic cells (FDC)[15]. In

mice, as much as 20% of the MZ B cells have been shown to shuttle between the marginal zone and follicle per hour.[16]

1.2.2 Positioning of MZ B cells in the marginal zone requires multiple signals

In rodents, MZ B cells were long believed to be sessile because they were only found in the marginal zone but not in the blood or other tissues. However, research has shown that MZ B cells can shuttle between the marginal zone and the follicles, sampling antigens from the blood and bringing them to FO B cells.[13,15,16]

Blood flow in the spleen is coming from an artery towards the marginal zone. There, the endothelial lining opens, which leads to a strongly reduced flowrate. The blood then continues towards the so-called red pulp and back into the circulation.[17] To be able to carry antigens from the blood to the follicles, MZ B cells have to migrate against the flow. Research investigating this movement has identified multiple adhesion molecules and receptors that allow MZ B cells to move into the follicle and back out again.

MZ cells are positioned at the marginal zone by the sphingosine-1-phosphate receptor 1 (S1PR1) signaling and CXCL13/CXCR5 signaling. [16,18,19]

After committing to the MZ B cell fate, the cells start upregulating S1PR1. Sphingosine-1 Phosphate (S1P) is a signaling molecule produced by red blood cells and is highly concentrated in the blood as well as the marginal zone.[20] Binding of S1P to S1PR1 leads to internalization of the receptor.[19,20] S1PR1 is necessary for MZ B cells to remain in the marginal zone, and after internalization of the receptor, the cells relocate to the follicle within ~30 min.[16] In the marginal zone, the cells adhere due to the present adhesion molecules α4β1and αLβ2 that bind VCAM-1 and ICAM-1.

MZ B-cells that are subjected to shear flow from the blood stream and are bound to the marginal zone through ICAM-1, start migrating towards the source of flow until they reach the endothelial lining of the marginal sinus, which is expressing MadCAM1 to which MZ B cells strongly adhere.[19,21] Cells at the endothelial lining and the follicle also express CXCL13 and MZ B cells bind to this via their receptor CXCR5. The CXCL13/CXCR5 signaling axis has been shown to facilitate entry of MZ B cells into the follicle.[15,18]

Taken together, this complex interplay of factors allows for accurate positioning of MZ B cells in the marginal zone and shuttling towards the follicles.

1.3 Factors involved in MZ B cell development

The development of MZ B cells and FO B cells is regulated by many signals.

1.3.1 BCR signaling intensity

BCR signaling intensity seems to have an important role in the FO/MZ cell fate decision. A study[22] reported, that mice lacking secreted sIgM have higher BCR signaling and show an increase in MZ B cells as well as a decrease in FO and T2 B cells. BCR signaling intensity was judged by the levels of phosphorylated (p-) downstream factors like Spleen Tyrosine Kinase (p-Syk), Bruton's Tyrosine Kinase (p-BTK) as well as expression levels of Nur77, a gene upregulated upon BCR signaling.[22] A different study[23] also suggested, that stronger BCR signaling is required for MZ B cell generation. The authors used mice with a transgenic BCR reactive to the self antigen Thy-1. In the presence of self antigen and therefore strong BCR signaling, the development of MZ B cells was preferred over FO B cell development. Finally, the authors of another paper[24] exchanged the cytoplasmatic IgM tail for an IgG tail and saw higher Ca^{2+} flux after BCR stimulation. They report an almost 10-fold increase in MZ B cell numbers, but also note that, apart from elevated Ca^{2+} mobilization, the induction of other BCR response genes was reduced.

In contrast, a different study[25] reported a decrease in MZ B cells upon higher BCR signaling. The authors reported, that knock-out mice of exon 2 of Sialate O-acetyl esterase (Siae) experienced higher BCR signaling, as judged by an increase in Ca^{2+} flux upon BCR ligation but showed a decrease in MZ B cell numbers.[25] Other studies[26] on the role of the transcription factor Aiolos (Ikzf3) also have shown increased Ca^{2+} mobilization in *Ikzf3*$^{-/-}$ mice after BCR stimulation and an absence of MZ B cells.

Taken together, it still remains to be elucidated how exactly BCR signaling intensity influences the MZ vs FO cell fate decision and if strong or weak BCR signaling is necessary for MZ B cell development.[27]

1.3.2 NF-κB signaling

NF-κB has been shown to be important for MZ B cell development.[28] The NF-κB signaling pathway consists of two sub-pathways. The classical/canonical and the alternative/non-canonical pathway. The classical pathway (NF-κB1) is triggered through receptors like TNF-αR or TLR's. Normally, the NF-κB1 dimers RelA and p50 are sequestered in the cytoplasm by the Inhibitor of κB α (IκBα). Upon stimulation, the IκB kinase complex IKK (consisting of IKKα, IKKβ and IKKγ) gets activated and phosphorylates IκBα, leading to its degradation. This frees RelA-p50 dimers to translocate to the nucleus and activate transcription of target

genes.[29] The alternative NF-κB2 signaling pathway is triggered through receptors like BAFF-R or lymphotoxin-β receptor (LTβR). This leads to the phosphorylation of the inhibitory p100 precursor via the kinases NF-κB–inducing kinase (NIK) and IKK. The phosphorylated p100 subunit then gets ubiquitinylated and processed into mature p52 which then translocates to the nucleus as a p52-RelB dimer.[30] There also seems to be some cross-talk between these two pathways.[29]

A study[31] with mice, that lacked p100 but still expressed the p52 form of NF-κB2, experienced constitutively active NF-κB2 signaling. These mice showed highly increased MZ B cell numbers while FO B cell numbers remained comparable to WT control.[31] The authors speculate, that this is due to increased survival of MZ cells, as judged by a significant decrease in cells that are Annexin-V5^{+}, an apoptotic cell marker. The increased survival was shown in vitro in LPS-treated as well as untreated cells. Knock-out of NF-κB2 (p100 and p52) resulted in a complete loss of MZ B cells and a reduction of FO B cells.[31]

Deubiquitinylating enzymes like Cylindromatosis (CYLD) have also been shown to play a role in MZ B cell development.[32] CYLD plays a role in negatively regulating various kinases of the classical and alternative NF-κB signaling pathway.[33] *CYLD*$^{-/-}$ mice experience increased NF-κB signaling and also showed an increase in MZ B cell numbers compared to WT. Interestingly, with increasing age of the mice, the proportion of MZ B cells in the spleen seemed to increase even further.[32]

A different study[34] also pointed towards the alternative NF-κB signaling pathway during MZ B cell development by analyzing RelB KO mice. These *Relb*$^{-/-}$ mice showed a complete loss of MZ B cells while having no effect on FO B cell numbers. Inactivation of other factors like cRel did not show this phenotype. The authors also studied the effect of double deletion of the upstream kinases IκBα and IκBε. Normally, *IκBα*$^{-/-}$ *IκBε*$^{-/-}$ mice show hyperactivation of the NF-κB pathway and die during the neonatal stage.[35] The authors rescued this phenotype by also deleting cRel and TNF. These *IκBα*$^{-/-}$*IκBε*$^{-/-}$ *cRel*$^{-/-}$ *TNF*$^{-/-}$ mice had normal B cell numbers and only experienced a decrease in T1 B cells, possibly due to an accelerated development. Importantly, they had highly elevated numbers of MZ B cells.

Taken together these studies point to the alternative NF-κB signaling pathway as a key driver of marginal zone B cell development.

1.3.3 MicroRNA miR146a

MicroRNAs (miRNAs) are a family of small non-coding RNAs that regulate gene expression by post-transcriptionally repressing target mRNAs via binding to partially complementary sequences in the 3'-untranslated regions (3'-UTR). This binding then recruits the so-called miRNA induced silencing complex (miRISC), which consists of proteins such as Argonaut or glycine-tryptophan repeat–containing protein of 182 kDa (GW182). Ultimately, binding of a miRNA to a target RNA leads to de-adenylation, de-capping and degradation of the target mRNA.[36]

The micro RNA miR146a is expressed in splenic tissue after NF-κB induction.[37] A recent study[38] analyzed the effects of miR146a on MZ B cell development. KO of miR146a resulted in an age-dependent decrease of MZ B cell numbers, where 8-week-old *miR146a*$^{-/-}$ mice had little to no MZ B cells compared to WT. At 12 weeks of age, the proportion of MZ B cells had increased, but was still lower than WT. Only after 18 weeks the numbers were comparable between *miR146a*$^{-/-}$ and WT. Importantly, FO B cell numbers were unaffected. The authors also report an increase in T1 and T2 cell numbers, suggestive of a developmental defect of transitional cells becoming MZ B cells. This defect, however, was not due to problems in B cell development in the bone marrow as B cell progenitor numbers there were similar to WT. The authors also did not observe a lack of retention of MZ B cells in the spleen or differentiation into plasma cells (PC). They did however observe decreased Notch2 activity in *miR146a*$^{-/-}$ B cells. Notch2 activity has been shown to be absolutely essential for MZ B cell development.[39] miR146a has sequence similarity to Numb, a negative regulatory factor of Notch2.[40] The authors propose a model, where miR146a decreases the levels of Numb, which then leads to increased Notch2 levels on the cell and increased generation of MZ B cells. However, these interactions between miR146a, Numb and Notch2 were not all shown in the same cell type, so further research is needed.

1.3.4 Notch2 signaling and ADAM10 protease

MZ B cell development is dependent of Notch2 signaling.[39,41–43] Binding of the ligand Delta-like-1(Dll-1) to Notch2 causes metalloproteinase and disintegrin-10 (ADAM10) to cleave Notch2 and γ-secretase to release the intracellular domain of Notch (NICD).[44] NICD then binds to the transcription factor RBP-Jκ and causes up-regulation of Notch target genes such as *Hes1*, *Hes5*, *Hey1* and *Dtx1* ultimately leading to MZ B cell differentiation.[45] *Hammad et.al.*[44] studied Taok3, a member of the Ste20 family of serine/threonine kinases. *Taok3*$^{-/-}$ mice lack MZ B cells and show lower Notch2 signaling compared to WT upon

stimulation by culturing on OP9 cells stably transfected with Dll-1. *Taok3*$^{-/-}$ mice also had lower levels of ADAM10^{+} B cells, but how exactly Taok3 causes the reduction of ADAM10 remains to be seen.

Adoptive transfer of ADAM10^{+} T1 cells into B cell deficient *Rag2*$^{-/-}$ mice showed, that the transferred cells almost exclusively become MZ B cells, while transfer of ADAM10^{-} T1 and ADAM10^{-} T2 cells gave rise to a mixture of FO and MZ B cells. The authors speculate that MZ B cells arising from these ADAM10^{-} T2 transferred cells might have upregulated ADAM10 after the transfer in vivo. This points to ADAM10 as a key factor involved in the MZ B cell fate decision.

A different study[46] showed that *Irf4*$^{-/-}$ mice experienced increased expression and activation of Notch2 which led to an increase of cells in the MZ. They attributed this to increased stabilization of intracellular Notch2. Injection of the therapeutic monoclonal antibody anti–negative regulatory region 2 (α-NRR2), which inhibits the activation of Notch2, led to a rapid loss of cells from the marginal zone. These cells did not undergo apoptosis but rather de-located to the blood. This shows, that continuous Notch2 signaling is necessary for retention of MZ B cells in the marginal zone and maintenance of a correct splenic architecture. Double knock-out of Irf4 and Taok3 rescued the decrease of MZ B cells seen in *Taok3*$^{-/-}$ mice.[44] Together, these studies show that Notch2 signaling is absolutely essential for MZ B cell development and maintenance and that key players involved in regulating Notch2 signaling also influence the MZ B cell compartment.

1.3.5 The transcription factor Aiolos (Ikzf3)

Aiolos (Ikzf3) is part of the Ikaros family of zinc-finger transcription factors.[47] Together these proteins play important roles in lymphocyte development and maturation.[48] A common feature of Ikaros family proteins is that they dimerize through two C-terminal C2H2 zinc fingers. They also appear to have multiple isoforms arising from alternative splicing. Together these factors represent a complex network with many interactions that influence lymphocyte development.[49]

Ikzf3$^{-/-}$ mice show an absence of MZ B cells while the FO B cell subset as well as the marginal zone architecture are normal.[26] Whether this is a B cell intrinsic process could not be addressed with the mice in this study. *Ikzf3*$^{-/-}$ lymphocytes have also been shown to experience enhanced BCR signaling.[26] Further insight into the interplay of Aiolos and BCR

signaling strength also came from studying Xid mice. Xid mice have a point mutation in Bruton's tyrosine kinase (BTK), an essential component of BCR signaling pathway, making it non-functional. This results in a roughly 50% reduction of mature B cells and a complete absence of subsets like B1 cells.[50] MZ B cells, however, are still present. *Aiolos*$^{-/-}$ Xid double mutants still have a MZ B cell subset, showing that Aiolos deletion can be rescued.[26] This indicates that both Aiolos and BCR signaling might influence MZ B cell development. The same study also analyzed other components of the BCR signaling complex like CD21. CD21 interacts with CD19 and this is believed to enhance BCR signaling by reducing the threshold of stimulation intensity required.[51] *Cd21*$^{-/-}$ mice have higher absolute numbers of MZ B cells but decreased numbers of FO B cells.[26] The authors propose that CD21 is a negative regulator of MZ B cell development, which is unexpected, as MZ B cells generally have higher surface CD21 levels than FO B cells. Also, CD19 has been shown to be a positive regulator for MZ B cell development, as *Cd19*$^{-/-}$ mice lacked MZ B cells.[52] How exactly Aiolos and BCR signaling intensity influence MZ B cell development and how CD21 and CD19 influence this needs further research.

In vitro, *Ikzf3*$^{-/-}$ B cells have been shown to proliferate better compared to WT when stimulated with anti-IgM.[48] Anti-IgM can bind to the BCR as well as FcγRIIB1, a low affinity receptor for IgG. The latter binding negatively influences the signaling response as it interferes with Ca^{2+} mobilization inside the cell.[53] To test whether Aiolos interferes with BCR signaling directly or rather enhances negative regulation through FcγRIIB1, the authors stimulated cells with $F(ab')_2$ fragments, which can only bind to the BCR. *Ikzf3*$^{-/-}$ B cells still showed a higher proliferative response than WT B cells, but less dramatic than with complete anti-IgM. This suggests, that Aiolos plays a role in negative regulation of BCR signaling.

1.3.6 Aim of this study

The aim of this study is to elucidate how Aiolos influences MZ B cell development. We have created conditional Aiolos KO mice that specifically delete in the B cell lineage, to analyze if the absence of MZ B cells is a B cell intrinsic phenotype. We also were able to rescue the loss of Aiolos by overexpressing Notch1 and we perform mRNA-Seq with these rescued Aiolos-deficient MZ B cells to identify Aiolos-regulated genes. To further analyze genes which are regulated by Aiolos we performed ChIP-Seq to identify binding sites of Aiolos in the genome. We further want to identify a mechanism how Aiolos influences BCR signaling strength, therefore we analyzed phosphorylation levels of various members of the BCR signaling

cascade. Taken together, this thesis provides insight into the function of Aiolos in B cells and serves as a basis for future experiments.

2 Results:

2.1 Characterization of Cd23-Cre mouse line

To study the mechanism of how Aiolos (Ikzf3) influences B cell development, we created germline deleted *Ikzf3*$^{-/-}$ as well as conditional *Ikzf3*$^{fl/fl}$*Cd23*-Cre mice that delete floxed alleles in the B cell lineage. Deletion of the *lox*P-flanked exon 8 (dimerization domain[49]) of Aiolos results in loss of Aiolos function and an in-frame addition of GFP (Figure 1A). Analysis of *Ikzf3*$^{-/-}$ mice with this GFP insertion shows that Aiolos is expressed from the pre-B cell stage onwards throughout the B cell lineage as well as in T cells, NK cells and monocytes (Figure 1B, left panel).

Previous studies of CD23-Cre mice suggested, that deletion happens as early as the immature B cell stage.[54] Careful analysis, however, showed deletion of Aiolos already in pre-B cells in the bone marrow. Even earlier deletion could not be assessed, since Aiolos was not expressed (Figure 1B, middle panel). To circumvent this, we also analyzed a *Rosa26* (*Rs26*) *Rs26*$^{LSL\text{-}YFP/+}$*Cd23*-Cre mouse where Cre mediated deletion leads to ubiquitous YFP expression. These data showed, that CD23-Cre deleted as early as the pro-B cell stage and also in various other cell types like monocytes, macrophages, granulocytes, NK cells, dendritic cells, and a small population of T cells (Figure 1B, right panel). This can potentially be explained by a very high chromatin accessibility of the *Rosa26* locus compared to the Aiolos locus and a slight "leakiness" of the Cd23-Cre allele, leading to premature deletion. Overall, these data show, that *Aiolos* is efficiently deleted by Cd23-Cre in the B cell lineage. Small populations of T cells, NK cells and monocytes are also deleted and expressing Aiolos.

2.2 *Ikzf3*$^{-/-}$ mice lack MZ B cells

We first analyzed the effect of *Aiolos* deletion on the B cell repertoire. As previously shown, *Ikzf3*$^{-/-}$ mice lack MZ B cells, but still have an intact FO B cell subset.[26] *Ikzf3*$^{fl/fl}$*Cd23*-Cre mice show the same phenotype, proving that this is a B cell intrinsic phenomenon (Figure 2A,B). We also noticed an increase in B1 cells in the spleen (Figure 3A). Analysis of unimmunized, 12-weeks-old *Ikzf3*$^{fl/fl}$*Cd23*-Cre mice showed no significant difference in germinal center (GC) B cells or plasma cells (PC) as described previously[48,55] (Figure 3B,C). Together these data show, that *Aiolos* deletion leads to a loss of MZ B cells and an increase in B1 cells while other subsets of B cells are unaffected.

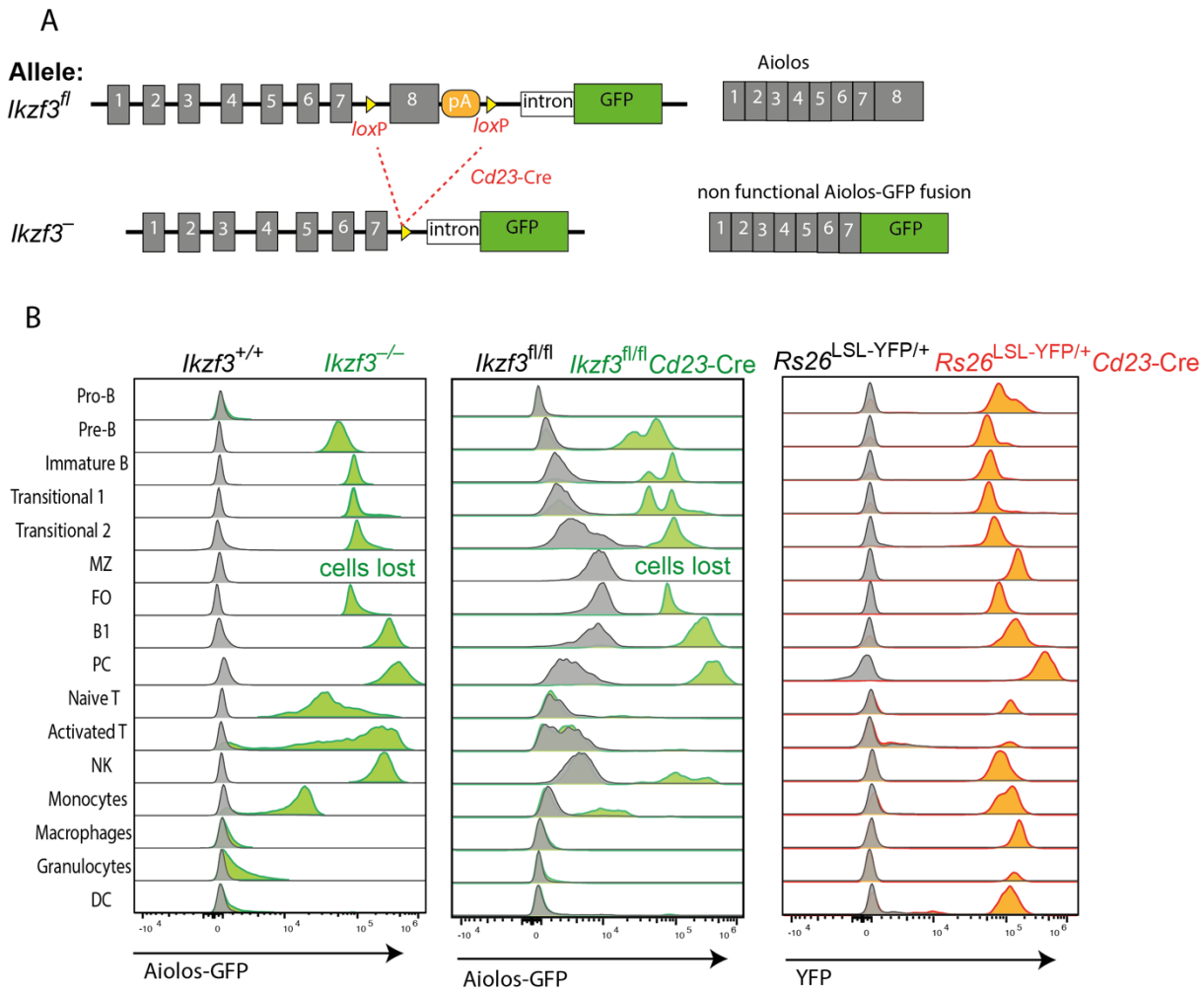

Figure 1: Aiolos is expressed in the hematopoietic system: A) Cre-mediated recombination of *lox*P sites leads to the deletion of exon 8 of Aiolos, which is necessary for dimerization and therefore function. The non-functional gene product has a GFP fusion. **B)** Expression of Aiolos throughout the hematopoietic system (left panel). Conditional deletion and expression are seen in B cells and a small percentage of T, NK and monocytes (middle panel). Conditional deletion of *Rs26*$^{LSL\text{-}YFP}$ (LSL: *lox*P-stop-*loxP*) shows, that deletion can occur to a high percentage as early as pro-B cells (right panel). However, this is probably due to an increased accessibility of the *Rosa26* locus compared to the *Aiolos* locus, as for example T cells are only deleted to a small extent in *Ikzf3*$^{fl/fl}$*Cd23*-Cre mice but where still expressing Aiolos. Each panel is derived from a single mouse. Data is representative of two experiments. For definition of cell types in flow cytometry see section Material and Methods.

Many publications showed that MZ B cell development is dependent on Notch signaling.[41–43] We next tried to see if ectopic Notch expression can rescue the MZ B cell compartment in Aiolos KO mice. We used a published[56] mouseline that comes with a flox-stop-flox cassette

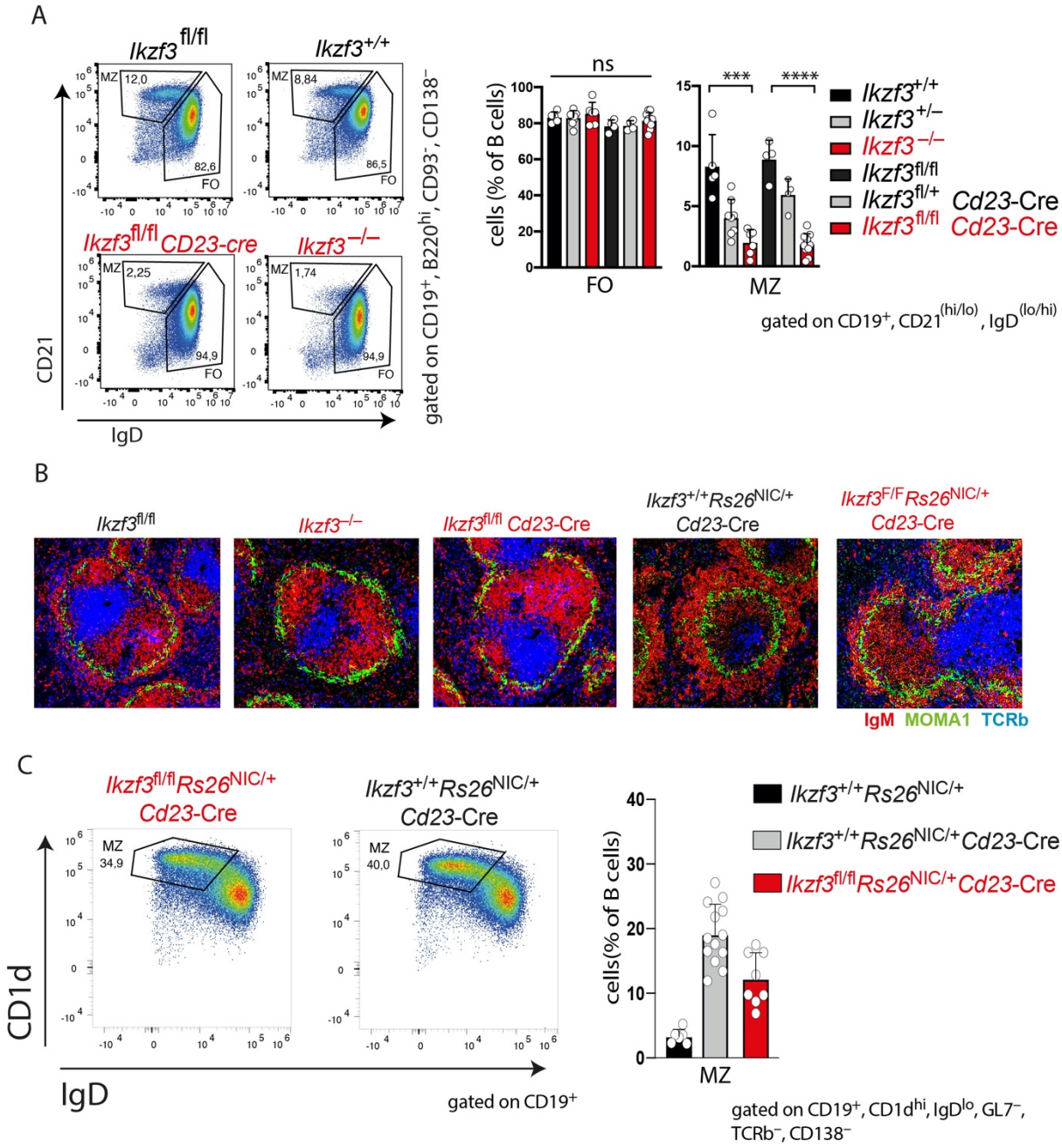

Figure 2: Conditional Ikzf3 deletion leads to a loss of MZ B cells: A) Conditional Aiolos deletion in B cells leads to the loss of MZ B cells, and this phenotype is identical to *Ikzf3*$^{-/-}$ mice. **B)** Histology of splenic architecture harboring Aiolos-deficient B cells and ectopic expression of the intracellular domain of Notch1 (NIC) **C)** Ectopic NIC overexpression through the *Rs26* locus leads to a rescue of MZ B cells. Plotted is mean ± s.d.
FO: One way ANOVA: ns (not significant) (P>0.05). MZ: *t*-tests, two tailed: P=0.0004(***), P<0.0001 (****).

upstream of the Notch1 intracellular sequence in the *Rosa26* locus. These *Ikzf3*$^{fl/fl}$*Rs26*$^{NIC/+}$*Cd23*-Cre mice show an increase in the proportion of MZ B cells in the spleen and this is even higher in *Ikzf3*$^{+/+}$*Rs26*$^{NIC/+}$*Cd23*-Cre mice, indicating only a partial

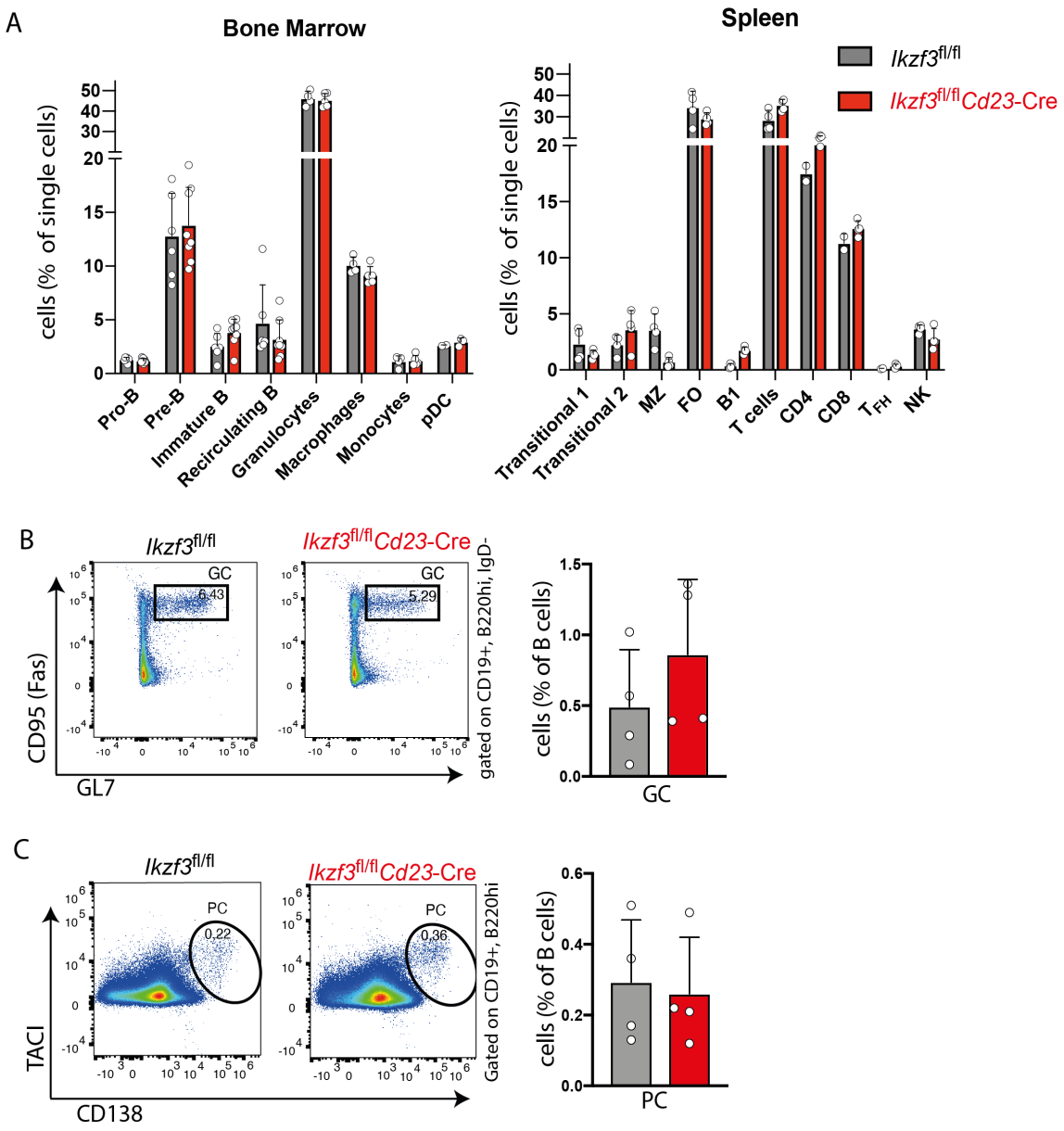

Figure 3: A) Hematopoietic lineages in conditional *Aiolos* KO and control mice. Conditoinal *Aiolos* KO mice have fewer MZ B cells and more B1 cells in the spleen. (See Figure 1A for a more detailed analysis on MZ B cells. The difference in B1 cells is also significant, but B1 cells are not part of this theses. **B) & C)** No difference in GC B cells and PCs is seen in unimmunized 12-week-old littermates. Plotted is mean ± s.d. Representative FACS plots are shown. Pre-gating strategy is indicated.

rescue and suggesting that Aiolos-deficient B cells have other defects in addition to Notch signaling (Figure 2B,C). Together these data show that Aiolos deletion leads to a loss of MZ B cells, which can be partially rescued by ectopic expression of the intracellular domain of Notch1 in B cells.

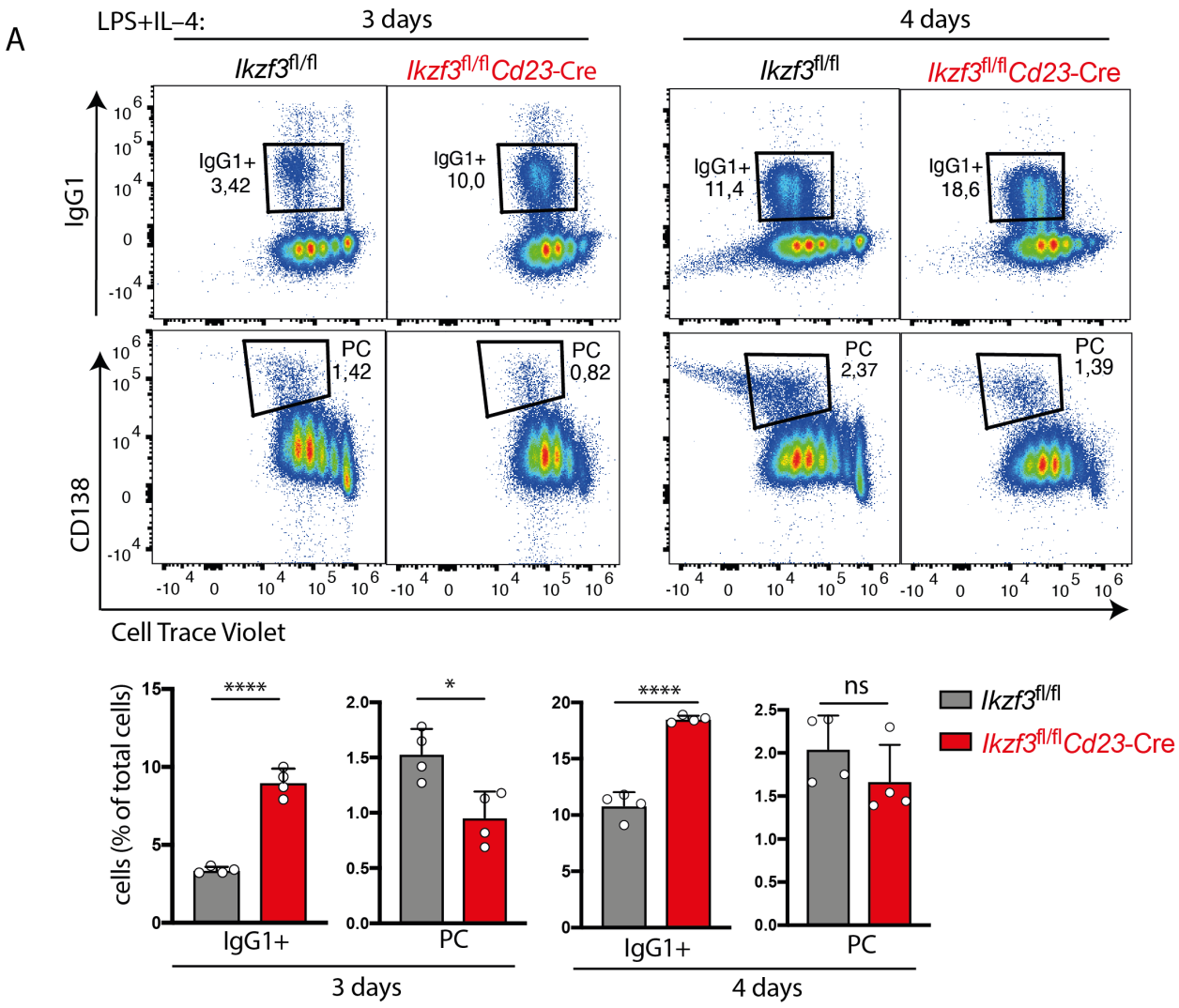

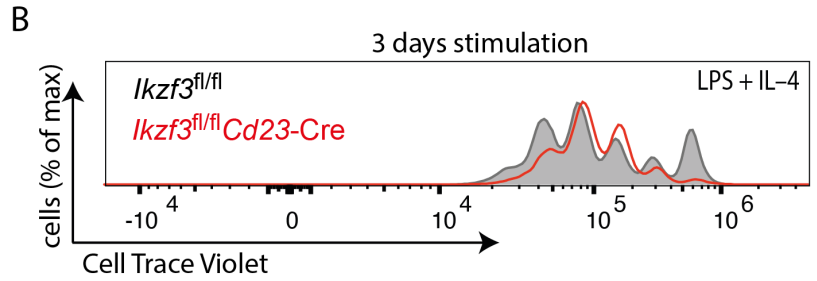

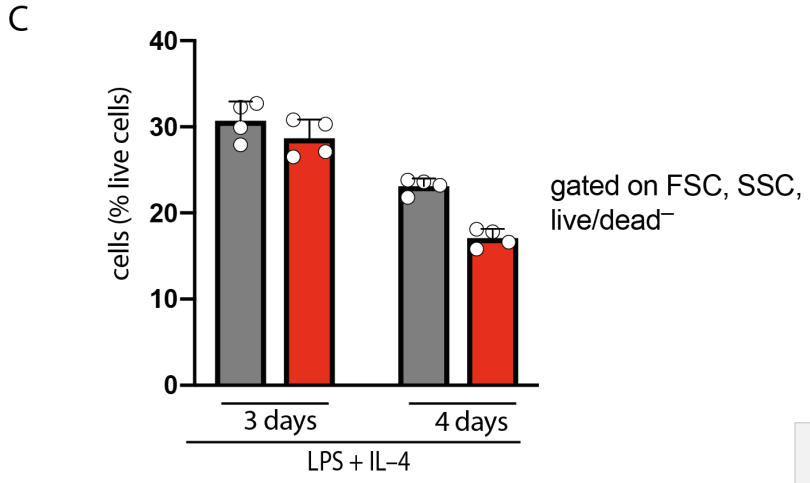

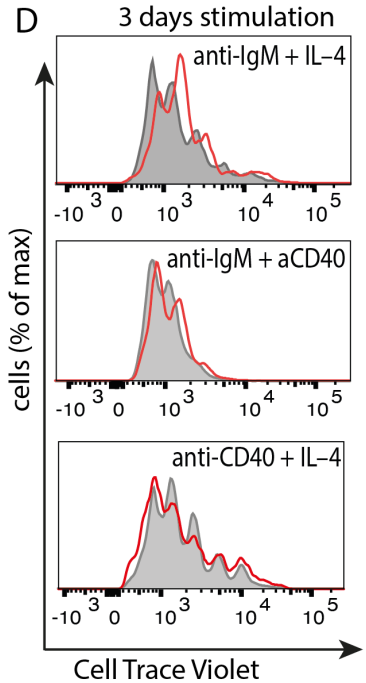

See next page for caption

Figure 4: In vitro class switch recombination: A) Stimulation of *Ikzf3*$^{fl/fl}$*Cd23*-Cre and control FO B cells with LPS + IL-4 in vitro for 3 days and 4 days. *Aiolos* KO B cells show enhanced CSR to IgG1 but reduced development into PC's. Representative flow cytometry plot and quantification is shown. **B)** Proliferation between Aiolos deficient and control FO B cells is similar in vitro after LPS+ IL-4 stimulation. Representative plot is shown. **C)** Viability of cells in vitro: Aiolos deficient FO B cells show lower survival in vitro after 4 days. **D)** Other stimulations tested also show similar proliferation between Aiolos deficient and control FO B cells but where not able to induce the formation of plasma cells or class switching to IgG1 or IgE (data not shown). Plotted is mean ± s.d. *t*-Tests, two-tailed: p<0.0001 (****), p=0.013 (*). ns: not significant.

2.3 *Ikzf3*$^{-/-}$ mice show increased class switching in vitro

To test for differences in the activation and stimulation of Aiolos-deficient B cells, we performed in vitro stimulation experiments. To this end, we purified CD43$^-$ FO B cells from lymph nodes of *Ikzf3*$^{fl/fl}$*Cd23*-Cre and control mice and cultured them in vitro with addition of LPS and IL-4 for 3 days or 4 days. While Aiolos-deficient FO B cells showed a higher percentage of class switching to IgG1, the generation of CD138$^+$ plasma cells was slightly reduced after 3 days and similar after 4 days, indicating that Aiolos-deficient FO B cells have a defect in PC development in vitro (Figure 4A). Importantly, the proliferation of the cells was unaffected by deletion of *Aiolos* (Figure 4B). Survival of the control and Aiolos-deficient B cells was similar at day 3 but slightly reduced after 4 days (Figure 4C). Other stimulations like anti-IgM+IL-4, anti-IgM+anti-CD40 and anti-CD40+IL-4 also showed no difference in proliferation (Figure 4D). These stimulations, however, did not cause class switching to IgG1 or IgE and also did not lead to the formation of plasma cells in vitro, neither in the control nor in the conditional *Aiolos* KO B cells (data not shown).

Together these data show, that Aiolos-deficient B cells undergo more efficient class switching to IgG1 but have defects in plasmablast development. They also show reduced in vitro viability compared to WT B cells.

2.4 ChIP-Seq and mRNA-Seq in control and Aiolos-deficient B cells

To identify factors that are deregulated in *Aiolos* KO mice, we performed chromatin immunoprecipitation combined with deep sequencing (ChIP-Seq) and mRNA-Seq in B cells.

In brief, for ChIP-Seq we harvested and CD43$^-$ depleted splenocytes from 2-week-old and adult mice, to get data for Aiolos binding in transitional B cells and FO B cells, respectively. We incubated the cells with formaldehyde and immunoprecipitated using either an anti-Aiolos antibody in C57BL6/J mice or with streptavidin beads in *Ikzf3*$^{bio/+}$*Rs26*$^{BirA/BirA}$ mice

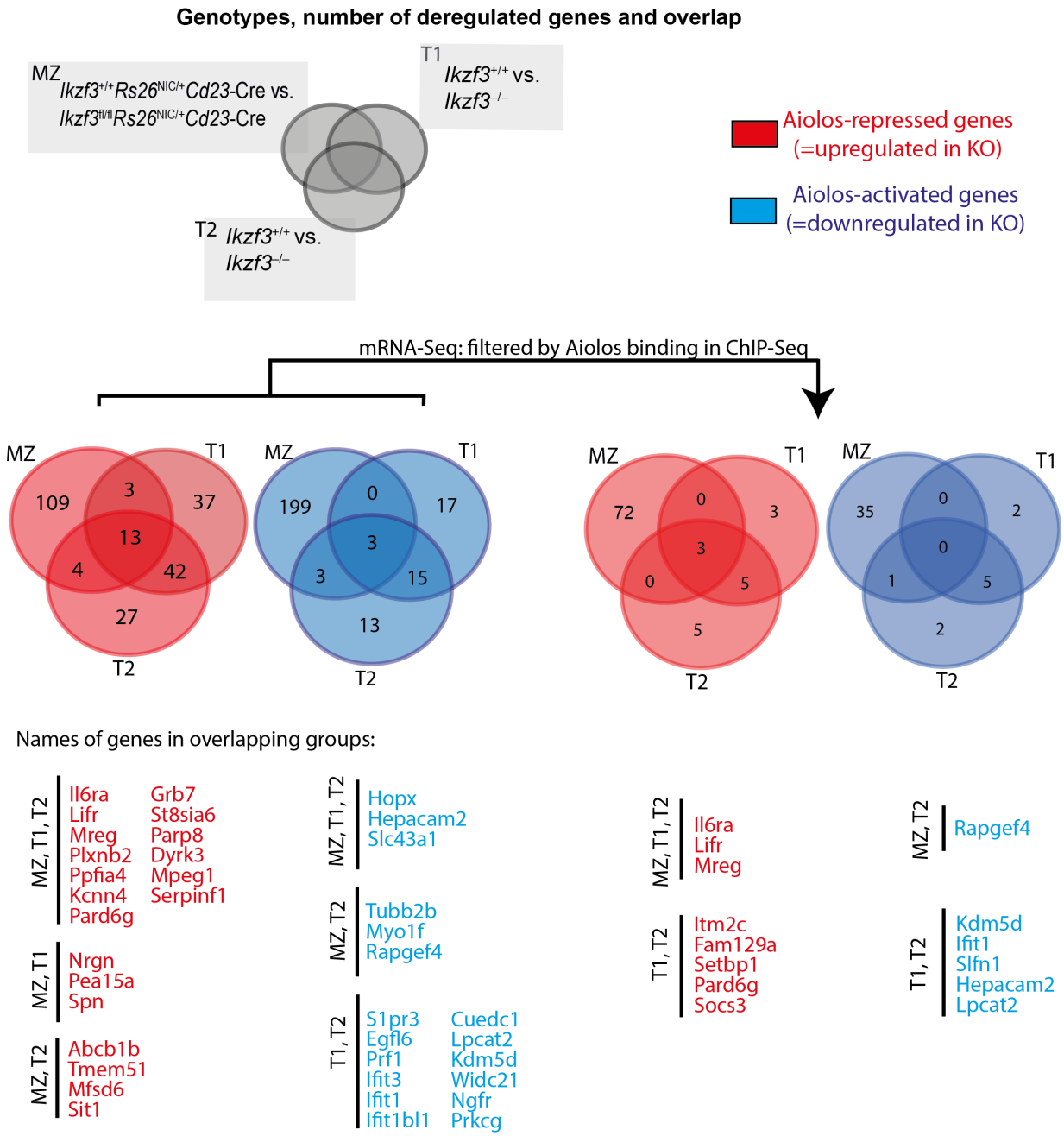

Figure 5: mRNA-seq and Aiolos-ChIP-Seq: Venn-diagrams indicate the number of differentially expressed genes between *Aiolos* KO and control B cells, filtered by the following parameters: FC>3, P_{adj} <0.05, TPM>5. Top: Indication of genotypes in each group. Red represents upregulated (=Aiolos repressed) and blue represents downregulated (=Aiolos activated) genes. Genes were then filtered by respective binding of Aiolos in ChIP tracks of FO B cells (see Materials & Methods for details). Indicated below are the names of overlapping genes.
MZ: *Ikzf3*$^{+/+}$*Rs26*$^{NIC/+}$*Cd23*-Cre vs *Ikzf3*$^{fl/fl}$*Rs26*$^{NIC/+}$*Cd23*-Cre from spleens from adult mice. T1 & T2: *Ikzf3*$^{+/+}$ vs *Ikzf3*$^{-/-}$ from spleens from 2-week-old mice.

See next page for caption

Figure 6: RNA-Seq in rescued MZ as well as transitional T1 and T2 B cells. MZ: *Ikzf3*$^{+/+}$*Rs26*$^{NIC/+}$*Cd23*-Cre vs *Ikzf3*$^{fl/fl}$*Rs26*$^{NIC/+}$*Cd23*-Cre from spleens from adult mice. T1 & T2: *Ikzf3*$^{+/+}$ vs *Ikzf3*$^{-/-}$ from spleens from 2-week-old mice. Colored red are upregulated (=Aiolos repressed) and blue are downregulated (=Aiolos activated) genes. Data shown is the mean from two replicates for each genotype. Example genes are labelled (see text). Cut-off for coloring: FC>3, P_{adj}<0.05, TPM>5.

that have a biotin-tagged Aiolos allele. For exact details see Materials and Methods. Of note, *Ikzf3*$^{bio/+}$*Rs26*$^{BirA/BirA}$ mice were analyzed for potential defects in the hematopoietic lineage due to the biotin tag but showed normal B cell development (data not shown). After ChIP we performed sequencing, followed by peak calling with MACS2 and peak to gene assignment.

For RNA-Seq, we sorted transitional T1 and T2 splenocytes of *Ikzf3*$^{-/-}$ and *Ikzf3*$^{+/+}$ mice as well as rescued MZ B cells from *Ikzf3*$^{fl/fl}$*Rs26*$^{NIC/+}$*Cd23*-Cre and *Ikzf3*$^{+/+}$*Rs26*$^{NIC/+}$*Cd23*-Cre mice. We purified the mRNA, followed by library preparation and NGS-sequencing. We then identified differentially expressed genes between T1, T2 and MZ B cells with DESeq2. We overlapped the differentially expressed genes between the datasets to find commonly deregulated genes and further filtered for genes that were bound by Aiolos in FO B cells. (Figure 5; Figure 6; Figure 8A).

This analysis revealed 13 genes that were commonly upregulated (Aiolos-repressed) in all three datasets and 3 of those were also bound by Aiolos. These genes include *Il6Ra* and *Lifr* which code for important cytokine receptors. Aiolos binding data in ChIP-Seq to these genes is shown (Figure 7A)**.** The upregulation of Il6Rα expression in the absence of Aiolos was also confirmed at protein level by flow cytometry (Figure 8B). To test for elevated cytokine signaling, we performed phosphlow experiments in transitional and FO B cells but could not detect elevated levels of phosphorylated STAT1, STAT3 or STAT5 (data not shown). However, we also saw gene upregulation of suppressor of cytokine signaling 3 (*SOCS3*) in T1 and T2 cells as well as *SOCS1* in MZ B cells, which could indicate a negative feedback loop. This potentially secondary effect might normalize cytokine signaling.

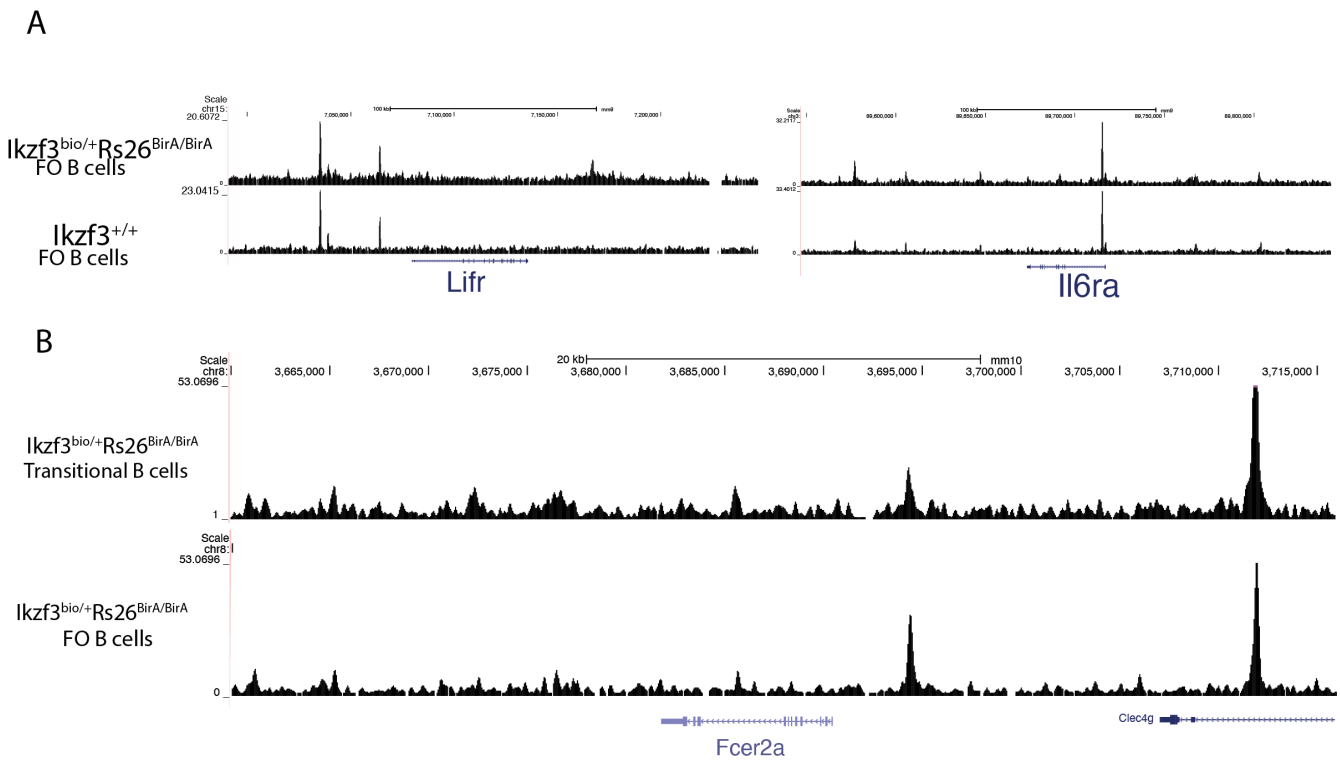

Figure 7: ChIP-Seq data for Aiolos binding: Aiolos ChIP was performed using an anti-Aiolos antibody in C57BL6/J (*Ikzf3*$^{+/+}$) mice as well as a biotin tagged version of Aiolos in *Ikzf3*$^{bio/+}$ *Rs26*$^{BirA/BirA}$ mice. **A)** Comparison of Aiolos binding in FO B cells between the two methods on selected example genes *Lifr* and *Il6Ra*. Binding profiles are similar. **B)** Comparison of Aiolos binding on *Fcer2a* (*Cd23*) in Transitional B cells and FO B cells. Binding is higher in FO B cells.

In Aiolos-deficient, NIC-rescued MZ B cells, *Tspan15* and *Tspan17* expression was decreased (=Aiolos activated) and *Adam10*-expression was slightly increased (=Aiolos repressed) (Figure 6; Figure 8A). Tspan15 and Tspan17 are part of the so called TspanC8 family of proteins and have been shown to regulate the activity of ADAM10, the key protease involved in the cleavage of Notch.[57–59] TspanC8 family members are believed to influence ADAM10 activity by regulating endoplasmatic reticulum (ER) exit and substrate specificity. However, Tspan15 has been shown to negatively regulate Notch signaling in various cell lines.[58]

Next, we sought to test the effect of Tspan15 on MZ B cells. To our knowledge, there are no functioning mouse Tspan15 flow cytometry antibodies available to directly measure the surface levels of Tspan15. We also wanted to measure ADAM10 levels on the cell surface by flow cytometry, but all available antibodies tested showed no measurable fluorescence signal (data not shown).

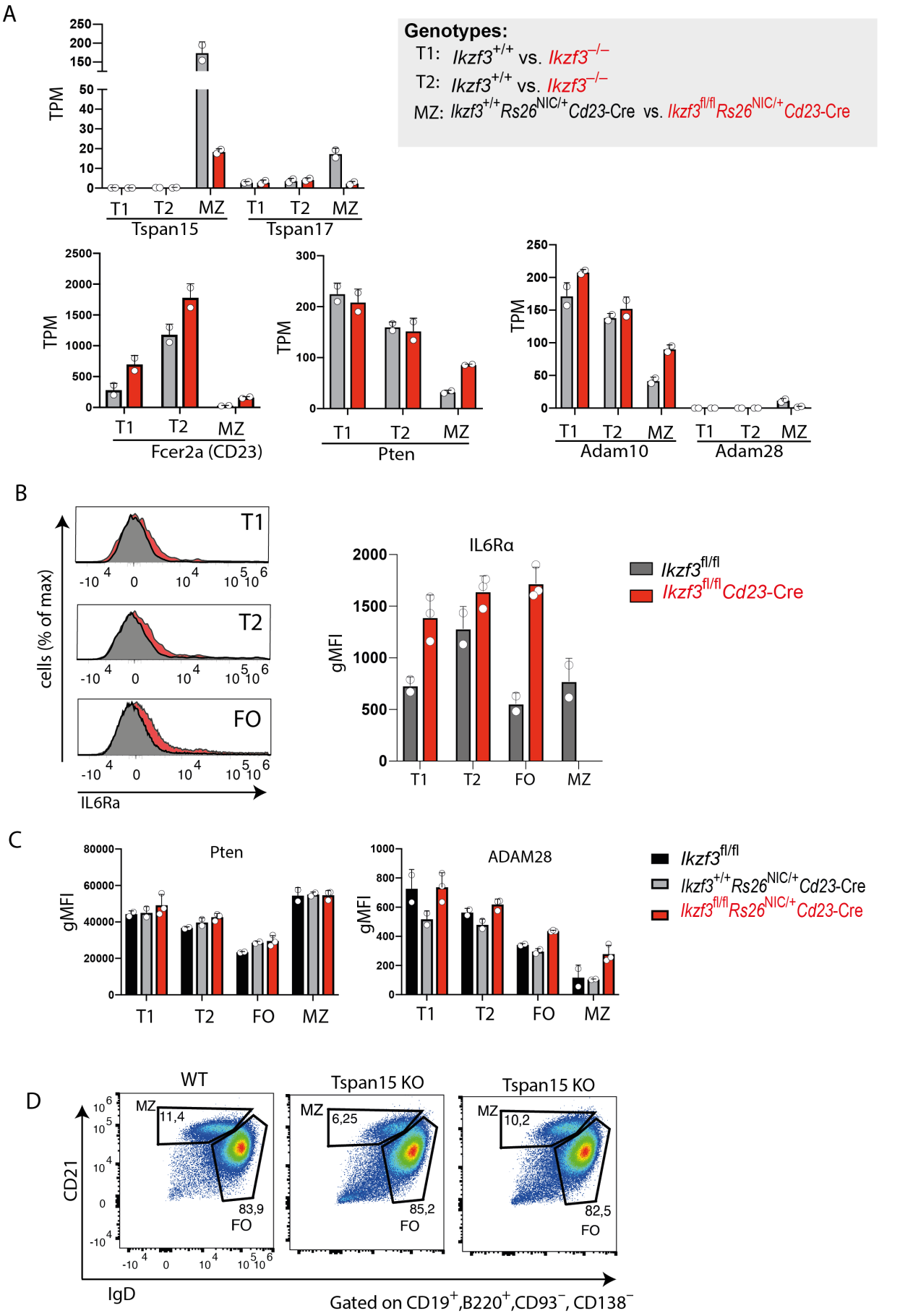

See next page for caption

Figure 8: Expression of selected genes and further validation: A) TPM values of mRNA-sequencing are shown. The following genotypes were used for differential gene expression: **MZ**: *Ikzf3*$^{fl/fl}$*Rs26*$^{NIC/+}$*Cd23*-Cre vs *Ikzf3*$^{fl/fl}$Rs26$^{NIC/+}$*Cd23*-Cre from spleens of adult mice. **T1 & T2**: *Ikzf3*$^{+/+}$ vs *Ikzf3*$^{-/-}$ from spleens from 2-week-old mice. **B)** Confirmation of IL6Rα protein levels by flow cytometry. *Aiolos* KO B cells have higher levels of IL6Rα. Representative histogram (left panel) and quantification are shown. No cells available for analysis of *Ikzf3*$^{fl/fl}$*Cd23*-Cre MZ B cells. **C)** Confirmation of Pten and ADAM28 expression levels by flow cytometry. While Pten levels are similar between all genotypes, ADAM28 levels are higher in Aiolos-deficient NIC-rescued MZ B cells compared Aiolos-sufficient B cells. **D)** *Tspan15* KO mice do not show an absence of MZ B cells. Plotted is mean ± s.d. Mice were kindly provided by Dr. Paul Saftig and his team (see main text for details).

We also analyzed the spleens from two Tspan15 KO mice, kindly provided by Prof. Dr. Paul Saftig and his team from the Biochemical Institute of the University of Kiel, Germany. Contrary to our hypothesis, these mice show no defect in MZ B cell development (Figure 8D). Together these data suggest, that Tspan15 is not a key factor in the development of MZ B cells.

Another deregulated protease is ADAM28, which has also been shown to be important for MZ B cell development by regulating Notch2 cleavage.[60] Analysis by flow cytometry showed that ADAM28 levels were higher in *Ikzf3*$^{fl/fl}$*Rs26*$^{NIC/+}$*Cd23*-Cre mice compared with *Ikzf3*$^{+/+}$*Rs26*$^{NIC/+}$*Cd23*-Cre mice, but similar to WT control mice (Figure 8C). Also, *Adam28* gene expression levels are around 100-fold lower than *Adam10* expression, making it unlikely to be the important member of the ADAM family of proteases in MZ B cell development (Figure 8A).

Other deregulated genes in Aiolos deficient B cells mice include *Pten*, which is expressed higher in NIC-rescued Aiolos-deficient MZ B cells, but is not differentially expressed in T1 or T2 B cells (Figure 8A). *Pten* KO mice have been shown to have an increased MZ B cell compartment.[61] However, analysis of Pten expression levels by flow cytometry showed no difference in Pten levels in Aiolos-deficient compared to Aiolos-sufficient NIC rescued MZ B cells (Figure 8C).

So far, we could not find an Aiolos-dependent gene that is required for MZ B cell development and therefore further analysis is required. Tspan15 was the most promising candidate, but two *Tspan15* KO mice analyzed showed no phenotype in the MZ B cell compartment.

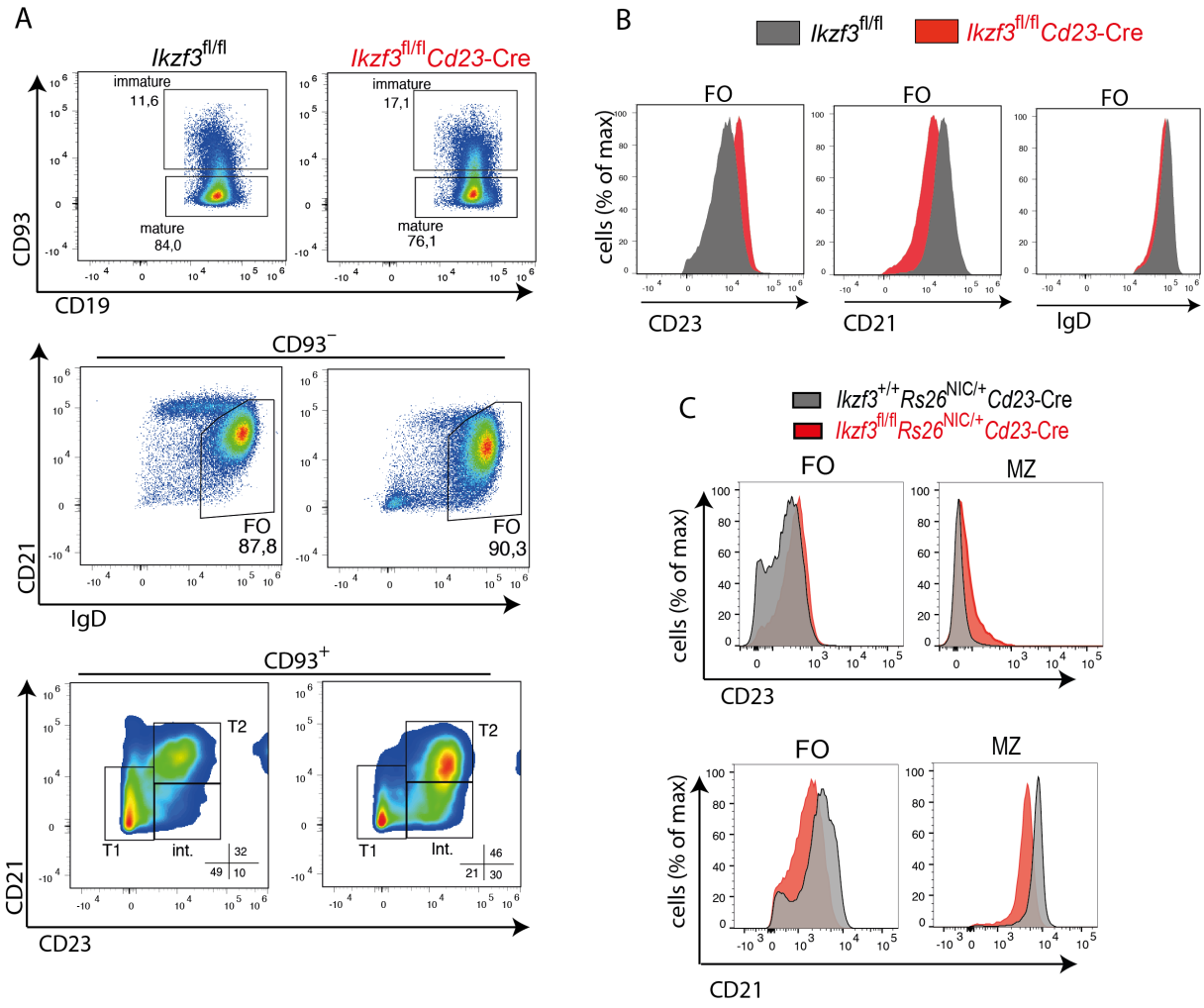

Figure 9: Deregulation of CD21 and CD23 in *Aiolos* KO mice: A) Gating strategy for mature and immature B cells in the spleen based on CD93 expression (top panel). Below are representative FACS plots showing mature ($CD93^-$) and immature ($CD93^+$) B cell populations. int. = Intermediate. CD23 deregulation is seen as early as the immature B cell stage. **B)** Representative histograms of CD23, CD21 and IgD levels in *Aiolos* KO FO B cells. IgD is not deregulated. **C)** NIC-rescued MZ B cells show similar deregulation of CD21 and CD23. See also quantification in Figure 10.

2.5 *Aiolos*-deficient B cells have deregulated CD23 and CD21 expression

We had noticed that Aiolos-deficient B cells express higher levels of CD23 and lower levels of the complement receptor 2 (CD21) (Figure 9; Figure 10A). This deregulation is also seen in $CD93^+$ transitional B cells, where a distinct population of $CD23^+CD21^-$ cells is seen that we termed intermediate (Int.), as it is in between the stages T1 and T2 (Figure 9A). Aiolos-deficient MZ B cells rescued by ectopic NIC expression also show elevated levels of CD23 and lower levels of CD21 (Figure 9C; Figure 10C), indicating that this deregulation is directly

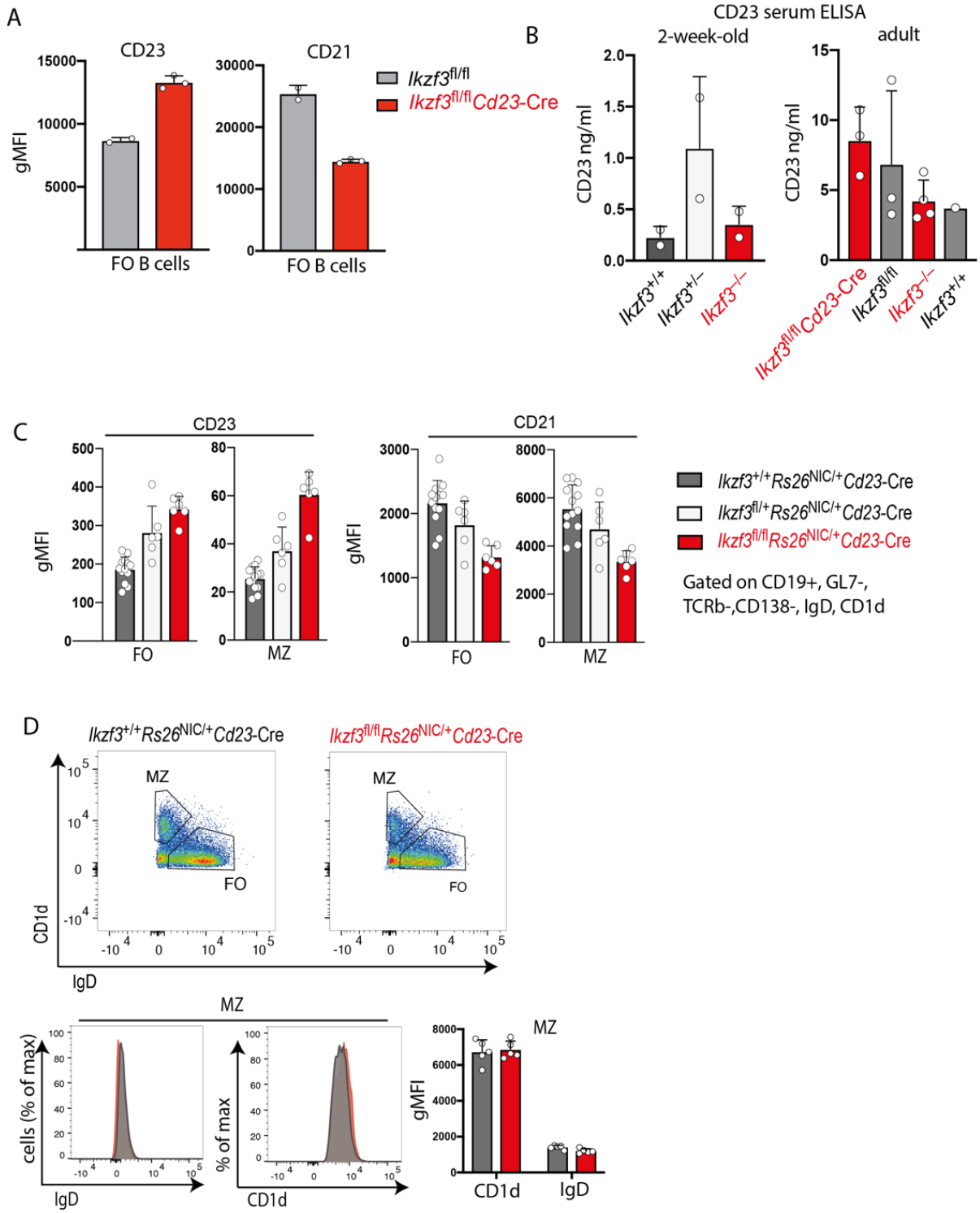

Figure 10: Quantification of of CD21 and CD23 deregulation : A) Quantification of CD21 and CD23 levels in Aiolos deficient and control FO B cells. **B)** Serum ELISA for CD23 in 2-week-old and mature mice. **C)** NIC-rescued Aiolos-deficient MZ and FO B cells still show the same CD21 and CD23 deregulation as seen in Aiolos-deficient FO B cells. **D)** NIC rescued Aiolos-deficient MZ B cells do not show deregulation of the other MZ specific markers CD1d and IgD. Representative histograms are shown. Plotted is mean ± s.d.

caused by the absence of Aiolos. Further ChIP-seq analysis showed that Aiolos was bound to the transcription start site (TSS) of *Fcer2a* (*Cd23*) and comparison of transitional and FO B

cells shows an increased binding in mature B cells (Figure 7B). Other key markers that are used to define MZ B cells like IgD and CD1d were not deregulated and therefore used for sorting strategies of MZ B cells (Figure 10D).

CD23 is shedded from the cell surface by ADAM10.[62] Although we were not able to directly analyze ADAM10 surface levels by FACS, we hypothesized, that a defect in shedding could also explain the increased surface levels of CD23. To test this, we performed ELISAs for CD23 in the serum from adult *Ikzf3*$^{fl/fl}$*Cd23*-Cre mice and 2-week-old *Ikzf3*$^{-/-}$ mice. However, *Aiolos* KO mice did not show lower serum CD23 levels. (Figure 10B).

Taken together these data show that Aiolos-deficient B cells have higher levels of surface CD23 and lower levels of CD21 surface expression which for CD23 is explained by differential gene expression rather than impaired shedding from the cell surface by ADAM10. Deregulation of CD23 and CD21 could influence BCR signaling. While CD23 has been shown to negatively influence BCR signaling[63], other studies showed that CD21 in complex with CD19 enhances BCR signaling.[51] Increased CD23 expression in combination with lower CD21 levels might dampen the BCR signaling capacities of Aiolos-deficient B cells.

2.6 Aiolos-deficient B cells have stronger BCR signaling

BCR signaling has been shown to be important for MZ B cell development, but there is conflicting evidence on whether higher or lower BCR signaling is necessary for the development of MZ cells compared to FO cells. To test this, we analyzed Ca^{2+} flux after BCR signaling by flow cytometry. In brief, we harvested lymph nodes from adult mice as well as spleens from 2-week-old mice, performed CD43^{-} depletion to obtain pure FO B or transitional B cells, respectively, and then stained cells with the Indo 1-AM calcium sensor dye. We then stimulated the cells with anti-IgM and analyzed the change in fluorescence by flow cytometry. Aiolos-deficient FO B cells showed an elevated Ca^{2+} response compared to WT control (Figure 11A). Baseline intensities were not significantly different. Preliminary results from transitional B cells also showed increased signaling in Aiolos KO transitional B cells (Figure 11B). However, further analysis is required. Consistent with previous studies[48], these data show that Aiolos-deficient B cells experience higher Ca^{2+} flux after BCR signaling.

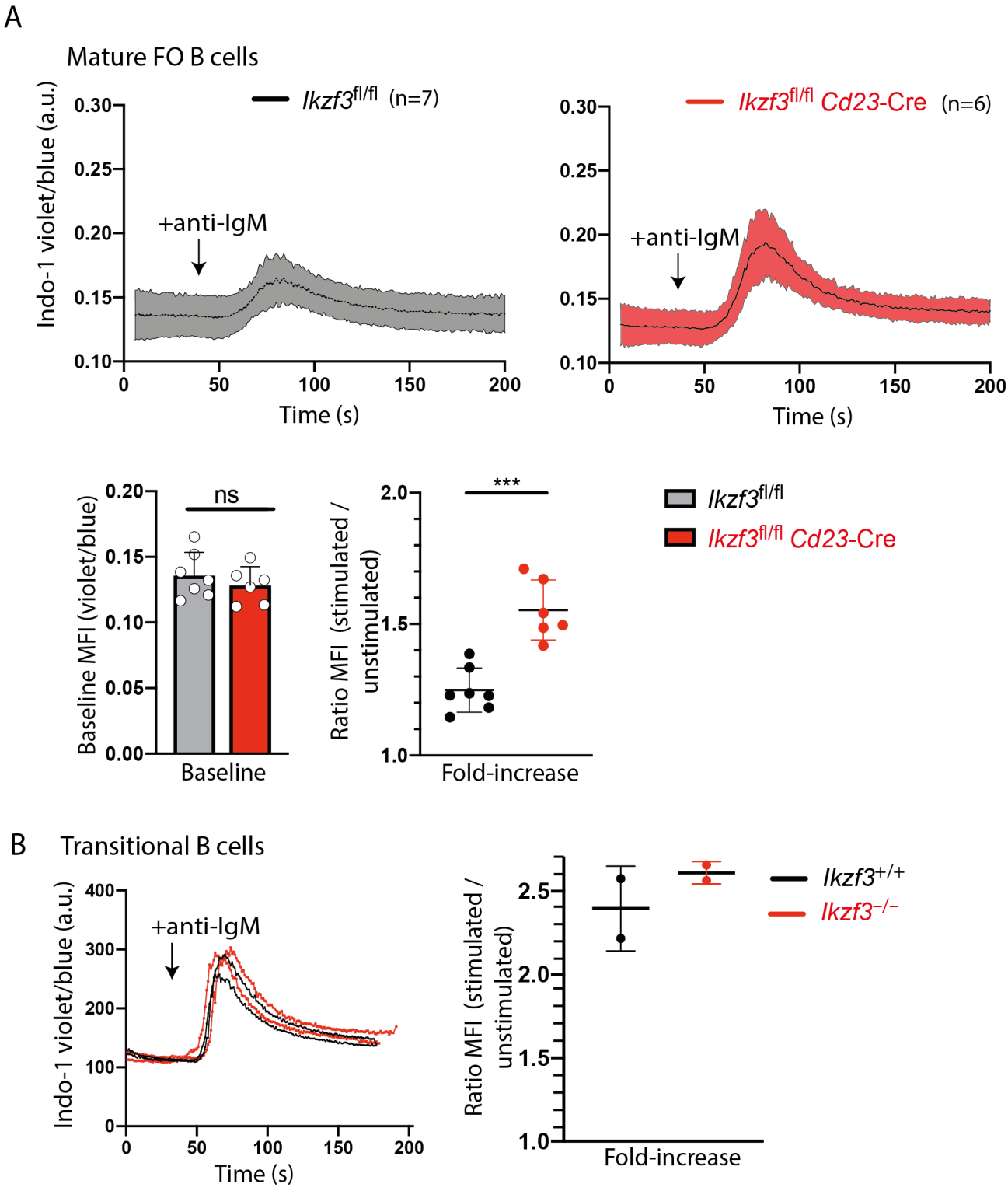

Figure 11: Aiolos deficient B cells have increased BCR signaling: A) Stimulation of mature FO B cells from lymph nodes of adult mice with 2.8µg/ml anti-IgM. The number (n) of replicates are indicated. Middle line represents mean, colored area shows ± s.d. **B)** Stimulation of transitional B cells from 2-week-old mice with the same concentration of anti-IgM as above. Each line represents one analyzed mouse.
Aiolos-deficient B cells have a higher fold-increase after anti-IgM stimulation, indicating stronger signaling. Baseline phosphorylations are not significantly different.
Plotted is mean ± s.d. T-tests, two tailed. p=0.0002 (***). a.u. = arbitrary units.

2.7 Aiolos KO mice have higher p-S6 levels

To further elucidate differences in BCR signaling, we analyzed phosphorylation levels of factors downstream of BCR signaling. For this, we again harvested lymph nodes from adult mice and spleens from 2-week-old mice and $CD43^-$ depleted them to obtain pure FO B cells and transitional B cells, respectively. These cells were then rested to reduce baseline phosphorylation levels of factors, that are generally thought to be influenced by the mechanical stress of tissue disruption.[64] We then stimulated the cells with anti-IgM $F(ab)'_2$ for 10 min and analyzed the levels of phosphorylation between Aiolos-deficient and control B cells.

Baseline phosphorylation levels before stimulation were not significantly different for most factors tested, with the exception of phosphorylated ribosomal protein S6 (p-S6). (Figure 12A,B; Figure 13A,B). The baseline levels of p-ERK and p-FOXO1/3 were slightly elevated, but these differences are not significant. After stimulation, we again saw higher levels of p-S6 and also p-AKT in mature and transitional B cells of *Aiolos* KO mice. Interestingly, phosphorylation of other factors in transitional B cells like BLNK, BTK, ERK, Syk or PLCγ2 were lower after stimulation compared with WT. Overall, these data point towards ribosomal protein S6 as a major deregulated factor.

Ribosomal protein S6 is phosphorylated by the S6 kinase 1 (S6K1) which is directly activated by mTORC1.[65] Elevated levels of p-S6 indicate an enhanced mTORC1 activity in Aiolos-deficient B cells. We analyzed two different phosphorylation sites of p-S6 (S235/236 and S240/244) that can be phosphorylated by S6K1[66] in transitional B cells and both showed elevated baseline as well as a higher increase upon stimulation in Aiolos-deficient B cells (Figure 14A). Importantly, a study[67] analyzed the effect of mTORC1 activity on MZ B cell development. The authors found, that upon loss of TSC1, a key negative regulator of mTORC1, mice showed elevated p-S6 levels and a complete loss of a marginal zone and MZ B cells. (for Model see Figure 14B) This could be reversed by treating *TSC1* KO mice with the mTOR inhibitor rapamycin.

These results lead us to the hypothesis, that increased BCR signaling in Aiolos-deficient B cells leads to higher mTORC1 activity and therefore p-S6 levels, which in turn negatively influence MZ B cell development.

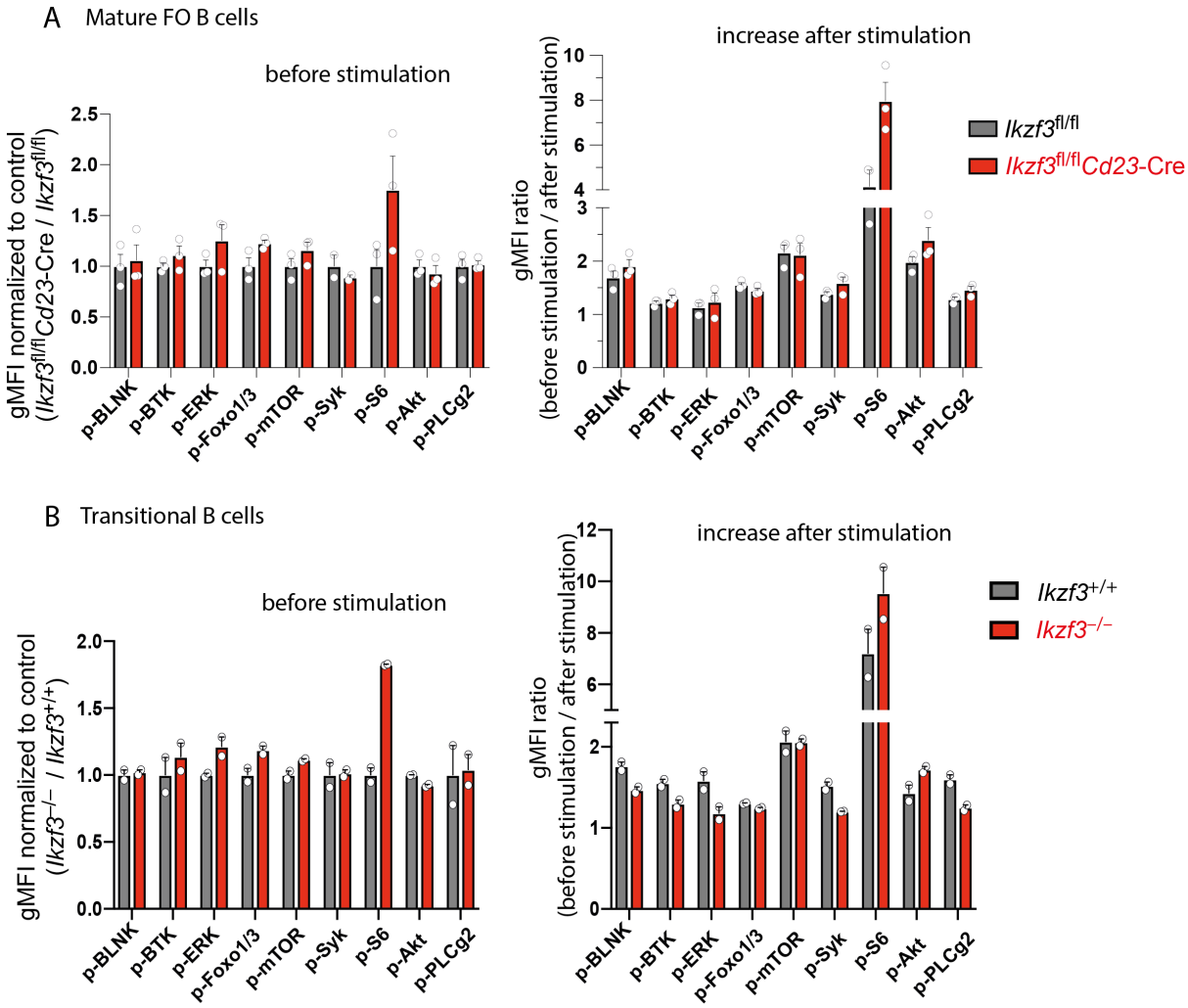

Figure 12: Phosphorylation levels downstream of BCR signaling: A) FO B cells from lymph nodes of adult mice and **B)** spleens from 2-week-old mice were harvested and CD43$^-$ depleted. Cells were rested and then stimulated for 10 min with 25µg/ml anti-IgM F(ab')$_2$ and analyzed by flow cytometry. Baseline phosphorylation levels (gMFI) are shown relative to the mean of WT control (baseline; left panels) and increase after addition of anti-IgM (peak/baseline; right panels). Purity was assessed to be at least 90% B cells. Potted is mean ± s.e.m. For information of phosphorylation sites and representative histograms also see Figure 13A,B.

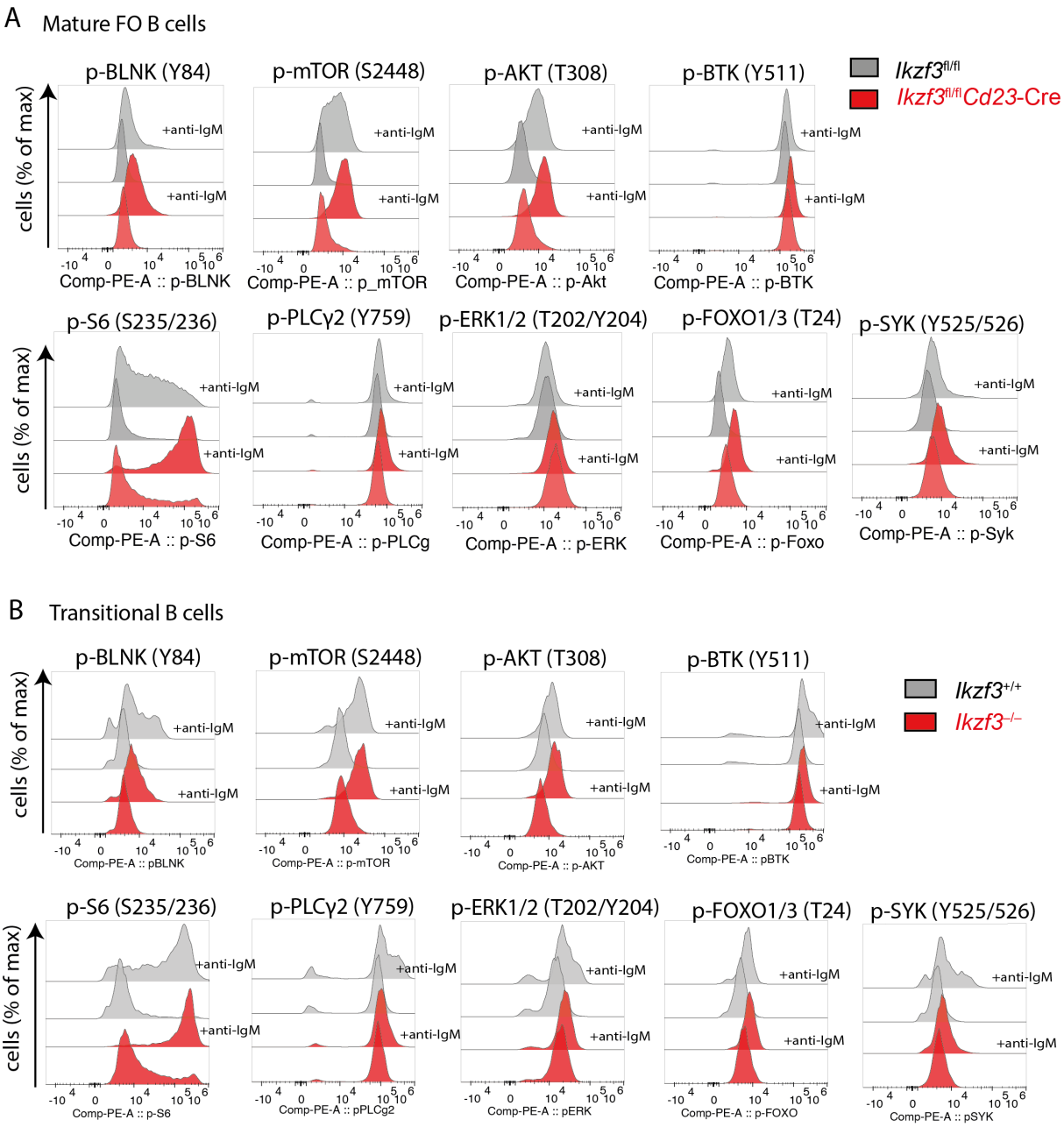

Figure 13: Representative histograms of phosphorylation levels of signal transducers after BCR stimulation with anti-IgM F(ab')$_2$: Factors downstream of BCR signaling are shown and phosphorylation sites are indicated in brackets. Cells were harvested from lymph nodes of adult **(A)** or spleens of 2-week-old mice **(B)**. CD43$^-$ depleted B cells were then rested to reduce baseline phosphorylation levels and then stimulated with 25µg/ml anti-IgM F(ab')$_2$ for 10 min. Purity was assessed to be >90% B cells. Histograms are representative examples of at least two experiments.

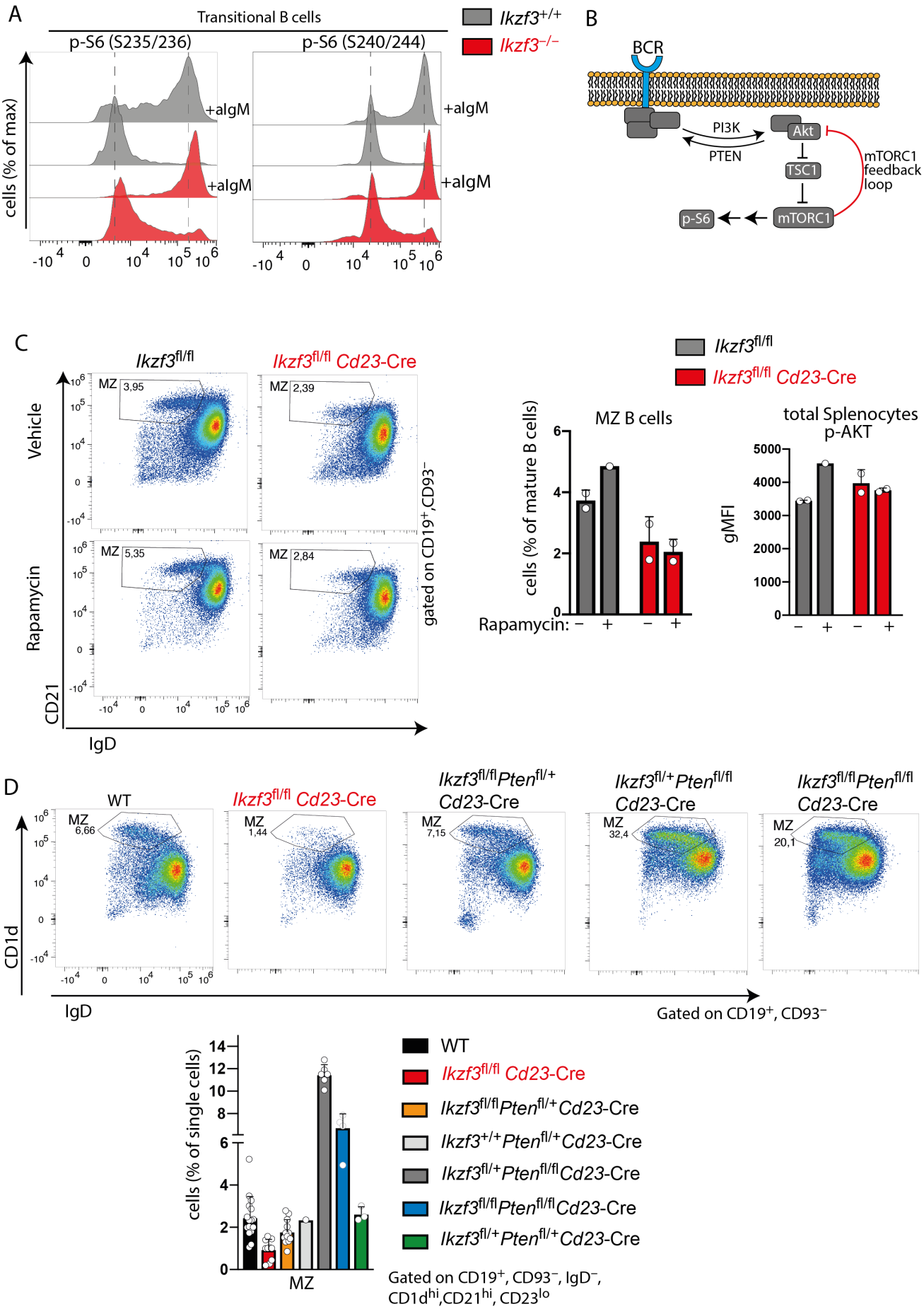

See next page for caption

Figure 14: The role of PI3K/AKT/mTORC1 signaling in MZ B cell development: A) Aiolos deficient transitional B cells have higher p-S6 levels, indicative of elevated mTORC1 signaling. Two different pairs of phosphorylation sites were analyzed. Representative histogram of two independent replicates is shown. **B)** Model of the PI3K/AKT/mTORC1 signaling including a negative mTORC1 feedback loop. **C)** Inhibition of mTOR through daily i.p. rapamycin treatment for 16 days leads to an increase in MZ B cells in WT but not in *Aiolos* KO mice. $CD43^-$ depleted B cells have differences in p-AKT levels: rapamycin treatment leads to increased p-AKT in WT. Vehicle treated Aiolos KO splenocytes have higher p-AKT but do not increase further upon rapamycin treatment, potentially indicating defective negative feedback loops. **D)** *Aiolos Pten* cDKO mice have MZ B cells, but the rescue seems to be only partial, as *Ikzf3*$^{fl/+}$*Pten*$^{fl/fl}$*Cd23*-Cre mice have more MZ B cells than *Ikzf3*$^{fl/fl}$*Pten*$^{fl/fl}$*Cd23*-Cre mice. This points to defects in MZ B cell generation outside of the Pten signaling axis.
Representative flow cytometry plots and quantification are shown. Plotted is mean ± s.d.

2.8 Rapamycin treatment does not rescue Aiolos-deficient MZ B cells

To further analyze the effect of p-S6 and mTORC1 signaling on the MZ B cell compartment, we treated *Ikzf3*$^{fl/fl}$*Cd23*-Cre and control mice with the mTOR inhibitor rapamycin or vehicle daily for 16 days. On day 17 we analyzed splenic B cells as well as the phosphorylation status of factors upstream and downstream of mTORC1.

Preliminary results show that rapamycin treatment can slightly increase the amount of MZ B cells in WT mice but fails to do so in Aiolos KO mice (Figure 14C). Interestingly, even vehicle treated conditional *Aiolos* KO mice show a slight MZ B cell compartment, which we cannot explain. Rapamycin treatment also led to a reduction in the amount of transitional B cells in both control and conditional *Aiolos* KO mice, potentially indicating a partial developmental block in early B cell development caused by the treatment (Figure 15A). Surprisingly, rapamycin treatment did not lead to a significant difference in p-mTOR, p-S6, p-PLCγ2 or p-FOXO1/3 levels (Figure 15B,C). However, p-AKT levels were increased in WT but not in Aiolos-deficient B cells, potentially indicating that negative mTORC1 feedback loops might be defective in the absence of Aiolos (Figure 14C). Negative feedback loops in mTOR signaling are for example the phosphorylation of Insulin Receptor Substrate (IRS) through S6K1, causing its degradation and altering its localization and thereby lowering p-AKT levels.[68] Other mechanisms involve the phosphorylation of the mTORC2 component Rictor through S6K1. This then leads to lower phosphorylation of AKT at serine 473 by mTORC2.[69] Defective negative feedback loops in Aiolos-deficient B cells could explain, why p-AKT levels are higher in the vehicle treated condition, but do not increase further by inhibiting mTORC1 with rapamycin treatment. This could also explain why Aiolos-deficient B cells have higher p-AKT levels upon BCR stimulation. (Figure 12A,B).

Together these preliminary data indicate that rapamycin treatment cannot increase the proportion of MZ B cells in conditional Aiolos KO mice but can do so in WT mice. In WT mice this is also accompanied by an increase in p-AKT levels, indicating that AKT signaling may be an important driver of MZ B cell development. However, this contradicts the observation, that Aiolos-deficient transitional and Aiolos-deficient FO B cells have higher p-AKT levels upon BCR stimulation but still lack MZ B cells. Further experiments have to be performed to precisely analyze the role of mTORC1 and AKT signaling in MZ B cell development.

2.9 Pten KO can rescue MZ B cells

Multiple papers have shown, that *Pten* KO mice have a highly increased MZ B cell compartment.[61,66,70] To further analyze the role of PI3K, Pten, AKT and mTORC1 signaling in the development of MZ B cells, we analyzed conditional *Aiolos Pten* double KO (cDKO) mice. *Ikzf3*$^{fl/fl}$*Pten*$^{fl/+}$*Cd23*-Cre mice have MZ B cells comparable to WT controls (Figure 14D). This shows, that *Aiolos* deletion can not only be rescued by ectopic NIC overexpression but also by lowering Pten levels. Lower Pten levels were also confirmed by flow cytometry (Figure 16A,B). Interestingly, when comparing homozygous to heterozygous *Aiolos* deletion in the *Pten* DKO setting, the rescue again was only partial as *Ikzf3*$^{fl/+}$*Pten*$^{fl/fl}$*Cd23*-Cre mice had more MZ B cells compared to *Ikzf3*$^{fl/fl}$*Pten*$^{fl/fl}$*Cd23*-Cre, pointing to additional defects outside of the Pten signaling axis. (Figure 14D)

We next wanted to analyze the phosphorylation status of various factors downstream of the PI3K/Pten signaling axis in B cells of *Aiolos Pten* cDKO mice. Surprisingly, phosphorylation levels of p-AKT and p-mTORC1 are only higher compared to WT in homozygous but not in heterozygous Pten deletion, even though the MZ B cell compartment was partially rescued in both genotypes. (Figure 14D; Figure 16A,B). Homozygous and heterozygous *Pten* KO mice have elevated levels of p-S6 and p-FOXO1/3. This is unexpected, because normally FOXO is thought to be directly negatively regulated by AKT.[71] This could, however, also be due to the deletion of *Aiolos* in these mice (Figure 12A,B).

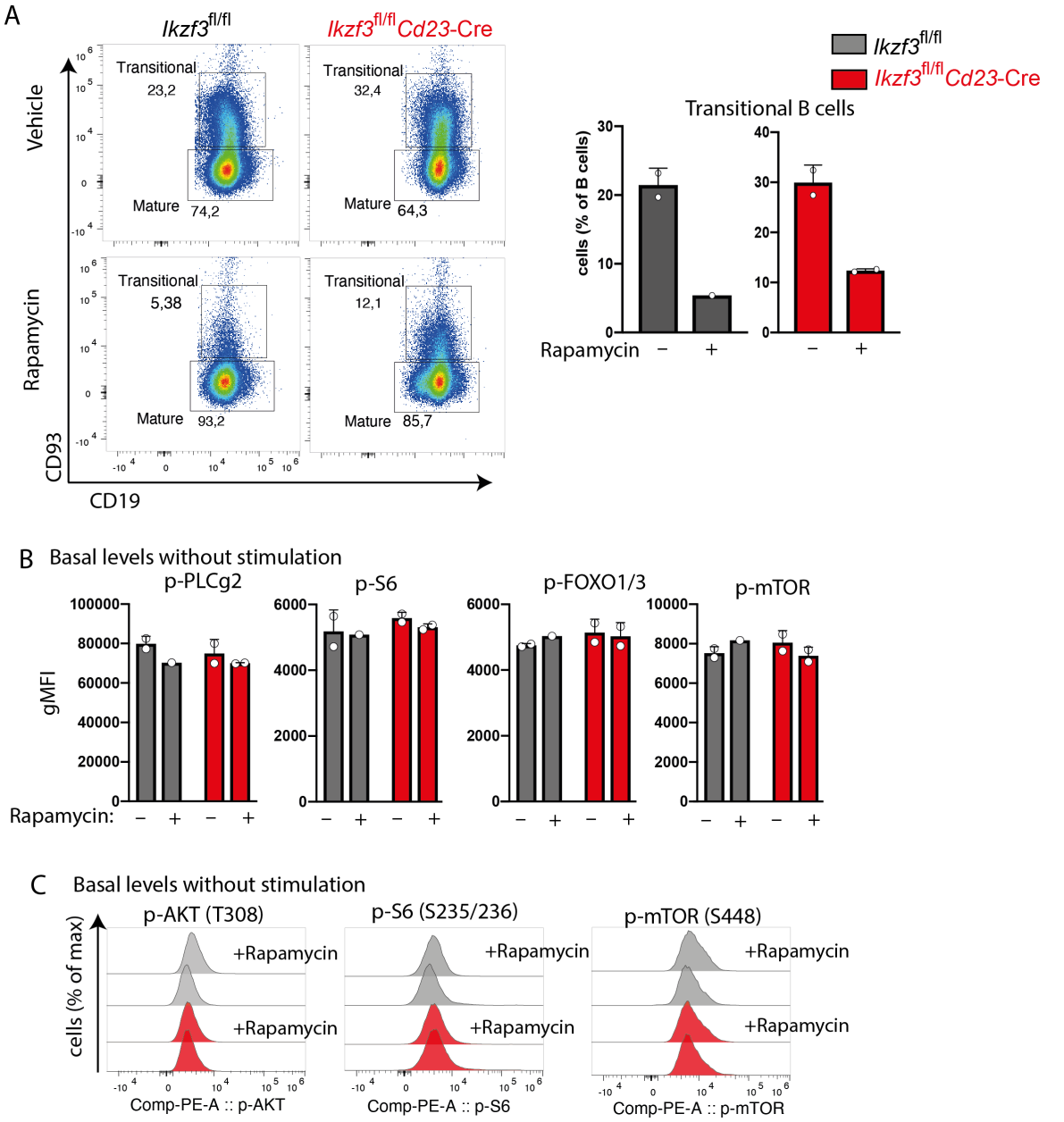

Figure 15: Treatment with rapamycin decreases the proportion of transitional B cells in the spleen: Rapamycin-treated mice have fewer transitional B cells, indicating a block in early B cell development. Of note, the conditional *Aiolos* KO and control mice were not at the same age, explaining the difference in the proportion in transitional B cells in the vehicle treated group. The mice within each genotype were littermates. This shows that rapamycin treatment reduced the amount of transitional B cells. **B)** Phosphorylation of selected proteins in total CD43⁻ depleted splenocytes. Treatment with rapamycin did not lead to drastic differences in p-PLCγ2, p-S6, p-FOXO1/3 or p-mTOR levels. **C)** Example of representative histograms of p-AKT, p-S6 and p-mTOR are shown. Phosphorylation sites are indicated in brackets.
The data are from CD43⁻ depleted B cells. Plotted is mean ± s.d.

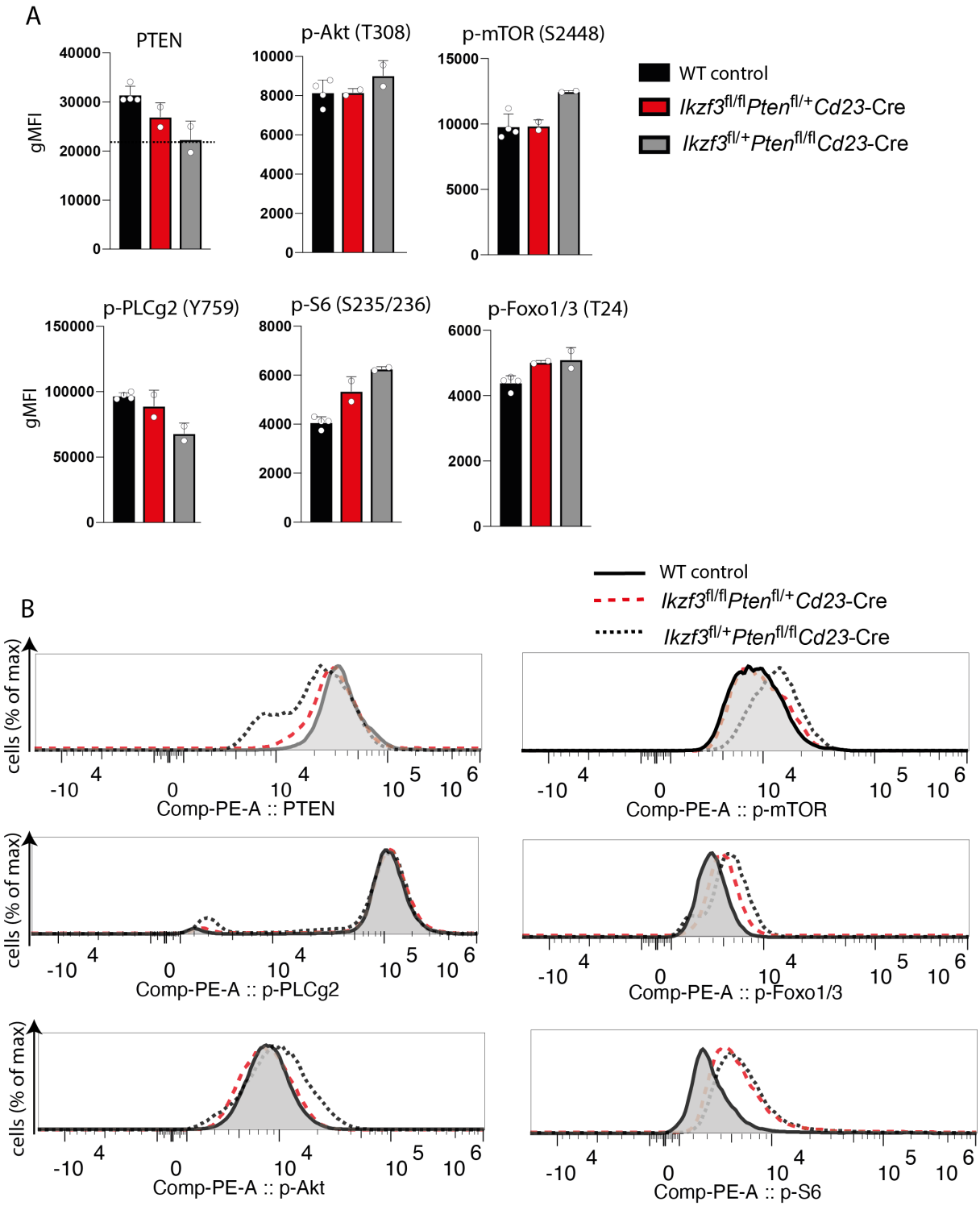

Figure 16: Phosphorylation levels of signal transducers in *Aiolos Pten* cDKO mice: A) Quantification of phosphorylation levels of signal transducers of B cells in *Aiolos Pten* conditional DKO mice by flow cytometry. Phosphorylation sites are indicated in brackets. Dotted line in first panel shows Pten KO levels **B)** Example histograms of phosphorylation levels that are representative of at least two experiments.
Data are from CD43⁻ depleted splenocytes. Plotted is mean ± s.d.

Together these data show that heterozygous Pten deletion can rescue the loss of Aiolos and lead to a normal size of the MZ B cell compartment. However, p-AKT and p-mTOR levels in *Ikzf3*$^{fl/fl}$*Pten*$^{fl/+}$*Cd23*-Cre B cells are not different compared to WT. This points towards other factors that may lie in the PI3K/Pten/AKT signaling network that may be important for MZ B cell development and are deregulated in *Aiolos* KO mice.

3 Discussion:

Based on *Ikzf3*$^{-/-}$ mice, Aiolos was previously described as a key regulator of MZ B cell development. Secondary effects of Aiolos deficiency in other hematopoietic cells could not be excluded in these studies. Here we use for the first time a conditional *Ikzf3*^{fl} allele that is specifically deleted in the B cell lineage to show that the loss of MZ B cells is a B cell-intrinsic phenotype.

Aiolos deficient MZ B cells can be rescued by increasing Notch signaling through ectopic overexpression of NIC, but this results only in a partial rescue as *Ikzf3*$^{fl/fl}$*Rs26*$^{NIC/+}$*Cd23*-Cre mice still have fewer MZ B cells than *Ikzf3*$^{+/+}$*Rs26*$^{NIC/+}$*Cd23*-Cre mice. This could be accompanied by additional defects other than Notch signaling defects in Aiolos-deficient B cells. However, it clearly shows that Aiolos-deficient MZ B cells can exist upon restoration of Notch signaling. A similar phenotype is seen in conditional *Aiolos Pten* DKO mice, where MZ B cell development is rescued, but *Ikzf3*$^{fl/fl}$*Pten*$^{fl/fl}$*Cd23*-Cre mice still have fewer MZ B cells than *Ikzf3*$^{fl/+}$*Pten*$^{fl/fl}$*Cd23*-Cre mice. This again points towards a partial rescue and a defect outside of PI3K/Pten signaling. It is therefore likely that Notch and BCR signaling defects together are responsible for the loss of MZ B cells in the absence of Aiolos.

To identify the molecular mechanism, by which Aiolos influences MZ B cells development, we analyzed signaling strengths after stimulation. We did see deregulation in CD21 and CD23 expression on the cell surface, which are involved in regulating BCR signaling strength.[51,63] Aiolos-deficient transitional and FO B cells had lower CD21 and higher CD23 levels and the same phenotype was seen in NIC rescued Aiolos-deficient MZ B cells. We also saw increased CSR upon LPS+IL-4 stimulation in vitro in Aiolos-deficient FO B cells as well as elevated Ca^{2+} levels after BCR stimulation with anti-IgM in Aiolos-deficient transitional and FO B cells. Previous studies predicted inconclusive results about the relationship between BCR signaling strength and the development of MZ B cells, but consistently with other authors, we show that Aiolos-deficient B cells experience stronger BCR signaling. We further analyzed differences in the phosphorylation of signaling factors downstream of BCR signaling, but

only saw minor differences, with the exception of higher p-AKT and p-S6.

S6 is phosphorylated by S6K1, which in turn is directly activated by mTORC1. A previous study showed that overactive mTORC1/p-S6 signaling plays a role in negatively regulating MZ B cell development and this could be reversed by rapamycin treatment.[67] Treatment of conditional Aiolos KO mice with rapamycin, however, did not lead to an increase in the proportion of MZ B cells in the spleen. The precise role that the PI3K/Pten/AKT signaling axis has in the development of MZ B cells remains to be elucidated.

We performed RNA-Seq of Aiolos deficient transitional T1 and T2 B cells as well as Aiolos deficient NIC-rescued MZ B cells. Commonly deregulated genes include *IL6Ra* and *Lifr*, but we did not see differences in cytokine signaling (data not shown), probably caused by upregulation of the negative regulators of cytokine signaling SOCS1 and SOCS3. We also saw differential gene expression of *Fcer2a* (CD23), which explains the higher levels of CD23 in Aiolos-deficient transitional and NIC-rescued MZ B cells.

The most promising result was the strong deregulation of Tspan15 seen in MZ B cells. Tspan15 is part of the TspanC8 family, which is involved in regulating the ADAM10 protease that cleaves Notch upon signaling. This would have provided a link between Aiolos expression and Notch signaling in MZ B cell development. However, spleens from *Tspan15* KO mice did not show any defect in their MZ B cell compartment. Unfortunately, we were not able to judge, if there are differences in the activity or the protein expression of ADAM10 in Aiolos-deficient B cells.

In conclusion, these data show that MZ B cell development is dependent on Aiolos, but loss of Aiolos can also be partially rescued by NIC overexpression or loss of Pten. Further studies are necessary to identify differentially regulated genes and differences in signaling cascades that might ultimately identify the molecular mechanism, by which Aiolos drives MZ B cell development.

4 Materials and Methods:

4.1 Generation of Aiolos KO mice

Aiolos KO mice were generated using conventional gene targeting methods. The presence of all alleles was confirmed by genotyping PCR's. C57BL/6J mice were maintained at our animal facility under specific pathogen free (SPF) conditions strictly following all guidelines for animal care. Unless otherwise noted, adult mice were analyzed after 8 weeks of age. To enrich for transitional B cells in the spleen, 2-week-old mice were also analyzed.
Of note, I*kzf3*$^{fl/fl}$*Rs26*$^{NIC/+}$*Cd23*-Cre mice develop T cell tumors (data not shown) after about 10-12 weeks of age, probably due to a slight leakiness of *Cd23*-Cre expression in T cells paired with NIC overexpression. Mice used for analysis were therefore strictly analyzed at 8-10 weeks of age before the onset of symptoms.

4.2 Flow Cytometry

All steps were performed on ice in FACS buffer [1xPBS, 2mM EDTA, 2% FCS] unless otherwise noted. For Flow Cytometry and cell sorting, we harvested spleen, lymph nodes (inguinal, brachial, axillary, cervical, mesenteric) or bone marrow (femoral), created a single cell suspension and performed red blood cell lysis by resuspending in ACK-lysing buffer (Gibco) for 1min at RT. The reaction was stopped by adding 5 volumes of cold FACS buffer. We then performed surface stainings on appropriate numbers of cells using the following anti-mouse antibodies in multiple commercially available colors (Supplier company in brackets): CD21 (BD), IgD (BD), IgM (BD), CD19 (BD), CD23 (BD), B220 (BD), CD1d (BD), CD93 (BD), IgG1 (various), IgE (various), TACI (BD), CD138 (Pharmingen), CD11c (BD), CD11b (BD), Gr1 (BD), cKit (eBioscience), CD95 (BD), CD115 (BD), CD62L (Biolegend), NK1.1 (Biolegend), CD5 (eBioscience), CD2 (BD) anti-Rabbit IgG (BD), CD126 (Il6Ra; BD), CD127 (IL7Ra; BD), LIFR (R&D systemsCD). ADAM28 (Bioss Antibodies, Cat. BS-5854R), Pten (CST, Cat. 9559S)
The following ADAM10 antibodies were tested but did not give satisfactory results: ADAM10-PE (R&D systems, Cat. FAB946P), ADAM10-APC (R&D systems, Cat. FAC946A)

For experiments, cells were stained in the dark on ice for at least 20min in the presence of Fc-Block and then washed to remove unbound antibodies.

For staining of intracellular Pten levels, 500k cells in 250ul FACS buffer were fixed by adding 1 Volume of 2x fixation buffer [final: 1.66% PFA, 0.1x Perm/Wash (BD, Cat. 554723)] for 15min at RT and then 30-60min on ice. After that, cells were washed twice with Perm/Wash, resuspended in 1ml Perm/Wash and incubated for at least 20min at RT to allow for complete permeabilization of cells. Subsequently, cells were stained in Perm/Wash with anti-Pten (1:100, CST, 9559S) for 1h at RT, washed twice and stained with 2nd anti-Rabbit-IgG-PE (1:1000).

Acquisition was performed on a Cytek Aurora spectral Flow Cytometer equipped with 355, 405, 488, 561 and 638 nm lasers and a total of 64 detectors. Sorting was performed on a FACS AriaIII (BD) equipped with 405, 488, 561 and 633nm lasers and a total of 16 detectors. Both instruments were provided and maintained by our Biooptics core facility.
Analysis was performed using FlowJo V10.7.

4.3 Definition of Populations in Flow Cytometry

Unless otherwise noted, the following surface markers were used to identify cell populations in Flow Cytometry. Indicated in brackets is the tissue, where cells were harvested. BM: bone marrow. Sometimes only a subset of these markers was used, if populations were still clearly distinguishable.

Pro-B (BM)	CD19+,B220+,IgD-,IgM-,cKit+, CD2-	**GC (spleen)**	CD19+, B220+, IgD-, CD95+,GL7+
Pre-B (BM)	CD19+,B220+,IgD-,IgM-,cKit-, CD2+	**Naïve T (spleen)**	TCRb+, CD19-, CD5+, CD44-, CD62L+
immature B (BM)	CD19+,B220-, IgD-,IgM+	**Activated T (spleen)**	TCRb+, CD19-, CD5+, CD44+, CD62L-
T1 (spleen)	CD19+,B220+,CD93+, CD23-,CD21-	**NK (spleen)**	CD19-, CD5-,Gr1-,NK1.1+
T2 (spleen)	CD19+,B220+,CD93+, CD23+,CD21+	**Monocytes (spleen)**	CD19-, NK1.1-, CD115+, Gr1-
MZ (spleen)	CD19+,B220+,CD93-, CD23-, CD21+,IgD-,CD1d+	**Macrophages (spleen)**	CD19-, NK1.1-, CD115+, Gr1+
FO (spleen)	CD19+,B220+,CD93-, CD23+, CD21-,IgD+,CD1d-	**Granulocytes (spleen)**	CD19-, NK1.1-, CD115-, Gr1+
B1 (spleen)	CD19+,B220-	**DC (spleen)**	CD19-, NK1.1-, Gr1-, CD11c+
PC (spleen)	CD19+,B220-, TACI+, CD138+		

4.4 B cell purification

B cells were purified in appropriate amount of FACS buffer (usually 100-200ul) supplied with 10% CD43-microbeads (Ly-48) (130-049-801, Miltenyi Biotec). Cells were incubated for at least 10min in the fridge and then isolated using a magnetic stand. Purity was confirmed to be at least 90% or higher.

4.5 Histology

For histological sections, spleens were harvested carefully and incubated on ice in the dark for at least 1h in freshly prepared 4% PFA in PBS supplied with 10% sucrose. For cryoprotection, organs were transferred to a 30% sucrose in PBS solution and incubated on ice for at least 3 hours. Organs were then embedded in optimum cutting temperature compound (OCT), frozen on dry ice and stored in -80C until use.
10-20um sections were cut using a microtome and fixed in Acetone. Sections were blocked in a humidified chamber at RT with 5% BSA and 10% mouse serum and stained with anti-TCRb-BV421, anti-IgM-APC and anti-CD169(MOMA1)-bio/SA-Cy3.
Sections were imaged on a Leica LSM780 Axio confocal microscope equipped with 400, 465 and 555 LED and spectral system combined with a high sensitive array of 32 GaAsP (Gallium Arsenide) detectors provided at our Biooptics Core facility. Overlaying and color correction of images was performed in Adobe Photoshop.

4.6 Ca^{2+} flux - BCR signaling

For Ca^{2+} flux after BCR stimulation, we first isolated B cells as described above. A small aliquot of cells from each sample was directly analyzed by Flow Cytometry to assess differences in fluorescence caused by the presence of GFP in Aiolos KO mice. The remaining cells were incubated in medium [IMDM, 10% FCS, 1% L-Glutamate, 1% Penicillin/ Streptavidin, 0.1% 2-ME.] supplied with 0.5uM Indo-1AM at a density of 4mio cells/ml. Roughly equal amounts of cells were used for stimulation. Cells were stained at 37C for 25min in the dark. Cells were then washed twice at RT to remove excess dye and further incubated in pure medium at 37C in the dark for 15min to allow for complete de-esterification of the dye, as recommended by the dye manufacturer. Stained samples were stored protected from light on ice and thawed around 12min prior to analysis.
Each sample was mixed and analyzed for 30s to obtain a baseline fluorescence reading. Afterwards, anti-IgM (prepared in-house) was added in flow to a final concentration of 2.8ug/ml and immediately mixed well. Fluorescence signal was acquired for roughly 4-5

minutes. Afterwards, Ionomycin was added as a positive control for signaling (data not shown). Between samples, the fluidics line was washed extensively with a total of 9ml H_2O using a fast-cleaning program. For each sample, 2 technical replicates were recorded. WT and KO samples were acquired in random order.

Analysis was performed using FlowJO V10.7. First, I calculated the ratio of fluorescence between 400nm (Ca^{2+} bound) and 480nm (not bound) and also subtracted differences caused by the presence of GFP. This was done by using the measurements of the so called "UV1" and "UV7" detectors available on our FACS system using the following formula: Ratio= (UV1 – $Baseline_{GFP}$)/ (UV7 – $Baseline_{GFP}$). The resulting derived parameter was plotted using the "Kinetics" tool in FlowJO. The median value of each technical replicate was exported. I then calculated the mean of both technical replicates of each sample. Average and s.d. of all WT and KO samples was then plotted using GraphPad Prism V8.0.2. The fold increase was calculated by dividing the maximum binding signaling fluorescence by the average not-bound baseline of the first 30s.

4.7 Analysis of protein phosphorylation levels by flow cytometry

For the analysis of phosphorylation levels of various proteins, we first isolated B cells as described above and purity was assessed to be at least 90% B cells. For stimulations, we split each sample in multiple aliquots. Cells were rested at a density of 5mio/ml in medium [1x 1640 RPMI, 2% FCS ,1% L-Glutamate, 1% Penicillin/ Streptavidin, 0.1% 2-ME] for 40min in a thermal shaker without shaking to reduce baseline phosphorylation levels of factors, that are known to be sensitive to mechanical stress.[64] We then added 1 Volume of stimulation in medium, mixed and incubated for 10min at 37C without shaking. To control samples we added pure medium. The reaction was stopped by adding 1Volume (=2x starting Volume) of fixation buffer [BD Cytofix, Cat. 554655, used as is; or eBioscience FOXP3/Transcription Factor staining buffer set, Cat. 00-5523-00, prepared as 2x in the provided Diluent]. Cells were incubated in Fixation buffer for at least 15min at 37C with shaking in the dark. Cells were then washed twice with 1xPerm/Wash buffer (BD Phosphlow, Cat. 557885 or eBioscience FOXP3/transcription Factor staining buffer set, Cat. 00-5523-00) and incubated in 1ml Perm/Wash buffer at RT for 20min in the dark to allow for complete permeabilization of cells. Cells were then aliquoted and stained in Perm/Wash buffer supplied with Fc-Block and Antibodies for 1h at RT in the dark with occasional, gentle mixing. Cells were washed twice and, where applicable, stained as before with anti-Rabbit-IgG-PE (1:1000) as secondary antibody and then analyzed using a Flow Cytometer.

Geometric mean fluorescent intensity (gMFI) of single cells were calculated. For Baseline plots (without addition of stimulation), each gMFI value was divided by the average gMFI of the Aiolos WT to show intensities relative to WT. For the increase plots, the gMFI of stimulated cells was divided by unstimulated to get the relative increase. Graphs were created using GraphPad Prism 8.0.2 and show mean ± s.e.m.

The following stimulation was used:
AffiniPure aIgM F(ab)'$_2$, 25ug/ml, (Jackson ImmunoResearch, Cat. 115-006-075)
The following antibodies were used:

Antibody	**Lot**	**Company, Cat. Nr.**	**Dilution**
p-BLNK-PE (Y84) Clone J117-1278	Lot: 6056930	BD, Cat. 558442	1:20
p-Syk-PE (Tyr525/526) (C87C1)	Lot: 4	CST, Cat. 6485S	1:50
p-AKT (T308) D26E6	Lot:7	CST, Cat. 13038	1:400
p-ERk1/2-PE (T202/Y204) Clone 20A	Lot: 5307895	BD, Cat. 612566	1:20
p-PLCγ 2-PE (pY759) Clone K86-689.37)	Lot: 7005720	BD, Cat. 558490	1:20
p-S6-PE (S235/236) D57.2.2.E XP	Lot: 10, 11	CST, Cat. 5316S	1:20
p-S6 (S240/244) XP DG8F8	Lot: 8	CST, Cat. 5364S	1:200
pBTK/ITK-PE (Y551/Y511) clone M4G3LN	Lot: E24645-101	eBioscience, Cat. 15557156	1:100
p-FOXO1/3a (T24/T32)	Lot: 7	CST, Cat. 9464S	1:200
p-mTOR-PE (S2448) clone MRRBY	Lot: 4307684	eBioscience, Cat. 12-9718-42	1:20
p-STAT1-PE (Y709) 58D6	Lot: 1	CST, Cat. 80625	1:20
p-STAT3-PE (Y705)	Lot: 83749	BD, Cat. 612569	1:20
p-STAT5-PE (Y694)	Lot: 7143633	BD, Cat. 562077	1:20
p-JAK2 (Y1007/1008)	Lot: 10	CST, Cat. 3771S	1:100

4.8 Rapamycin treatment

Appropriate amount of rapamycin (MedChemExpress, AY-22989) was dissolved in pure EtOH and then diluted in 1xPBS (final 10% EtOH). The suspension was mixed, aliquoted and frozen in -80C until use. Mice were injected i.p. with 75ug rapamycin or Vehicle as control

daily for 16 days. Mice were sacrificed and analyzed on day 17. The rapamycin suspension was thoroughly mixed before every loading into the needle to ensure equal administration across all mice.

4.9 In vitro Stimulation for CSR

Lymph Nodes (inguinal, brachial, axillary, cervical, mesenteric) were harvested and B cells isolated as described above. Cells were washed once with PBS and then stained at a density of 6mio cells/ml with 2.5uM cell trace violet (Thermo, Cat. C34557) in PBS+0.1% BSA for 7min at 37C. Reaction was stopped by adding 10 Volumes of medium [RPMI, 10% FCS, 1% L-Glutamate, 1% Penicillin/ Streptavidin, 0.1% 2-ME] and incubating for 5min.
Cells were washed and plated at a density of 1mio cells/ml in 24-well plates and stimulated with cytokines for 3 days or 4 days at 37C, 5% CO_2 using the following cytokines (LPS: 25ug/ml, IL-4: home made; concentration unknown: used as 1:2000). Stimulations with other combinations of cytokines, including aCD40 (2ug/ml) and aIgM (2.8ug/ml) were also performed for 3 days the same way and analyzed on a BD LSR Fortessa 2, resulting in different cell trace violet intensities seen in Figure 4B,D.
To exclude dead cells, additionally to other surface markers we stained cells with a fixable viability dye eF780 (Thermo) before analysis.

4.10 ChIP-Seq

For ChIP in FO B cells, spleens from adult C57BL/6J mice and *Ikzf3*$^{bio/+}$*Rs26*$^{BirA/BirA}$ mice, that have a biotin tagged Aiolos were harvested and CD43 depleted as described above. ChIP tracks between C57BL/6J and biotin tagged Aiolos were performed as replicates and are highly similar. Of note, *Ikzf3*$^{bio/+}$*Rs26*$^{BirA/BirA}$ mice were analyzed for defects in the hematopoietic lineage due to the biotin tag, but none were found (data not shown).
For ChIP in transitional B cells, spleens from 2-week-old *Ikzf3*$^{bio/+}$*Rs26*$^{BirA/BirA}$ mice were harvested as described above.
Cells were counted and at least 50-100mio cells were used for ChIP.
Fixation: Cells were fixed in 1% PFA for 10min at RT in FACS buffer and reaction was quenched by adding 1/3 Volume 2.5M Glycin and incubating shortly at RT. Cells were then centrifuged and washed twice with ice cold PBS.
Nuclei preparation: All steps were carried out at 4C and all buffers were supplied with cOmplete protease inhibitors (Roche). Cells were incubated at 4C with gentle rotation for 10min in buffer A [10mM HEPES ph=8, 10mM EDTA, 0.5mM EGTA, 0.25% TritonX100] followed by 10min in ice cold buffer B [200mM NaCl, 10mM HEPES ph=8, 1mM EDTA,

0.5mM EGTA, 0.01% TritonX100] both at a density of 2mio cells/ml. Nuclei were then lysed in chromatin lysis buffer [200mM NaCl, 50mM Tris/HCl pH=8, 10mM EDTA, 0.25% SDS] for at least 30min at 4C at a density of 25mio cells/ml.

Sonication: Chromatin was sonicated to fragments around 400-1000bp in length. Sample was centrifuged at 15.000g for 20min at 4C to remove any debris. Concentration of chromatin was measured by Nanodrop and chromatin was diluted 2.5x in Chromatin-dilution buffer [250mM NaCl, 1.67% TritonX100] (1ml sample + 1.5ml buffer) to bring down the SDS concentration to 0.1%.

One of the following protocols for immunoprecipitation was followed:

Biotin-Streptavidin-Immunoprecipitation: per 400ug of Chromatin, 15ul Streaptavidin Mag Sepharose beads were used. Beads were washed with TE and blocked in 10% BSA 10% PVP for 10min. 1% of Chromatin was saved as input. The rest was incubated with the beads o/n 4C with rotation. Beads were then washed by incubating for 5min at RT with rotation: twice in buffer S1[0.5M LiCl, 1mM EDTA, 1% Nonidet P-40, 1% Na-deoxycholate], three times with S2 [10mM Tris/HCl pH=8, 1mM EDTA, 3% SDS], twice with TE, once with high-salt buffer [10mM HEPES ph=7.9, 20% Glycerol, 700mM KCl, 2mM $MgCl_2$, 2mM 6AA, 0.5mM DTT, 0.2% Nonidet P-40], once with LiCl buffer [250mM LiCl, 50mM Tris/HCl ph=8, 0.5% Na-deoxycholate, 1% Nonidet P-40] and twice with TE. After the final wash buffer, the beads were resuspended in 300ul elution buffer [10mM Tris/HCl pH=7.5, 1mM EDTA, 1% SDS, 100mM $NaHCO_3$ (fresh), 200mM NaCl] and Proteinase K was added to a final concentration of 300ug/ml. Elution buffer and Proteinase K were also added to the input chromatin. Both samples were incubated o/n at 55C to reverse the crosslinking. The DNA was then purified using the ChIP DNA Clean & ConcentratorTM Kit (Zymo research D5205) according to the manufacturers protocol.

Antibody Immunoprecipitation: Per 400mg of chromatin 10ul Protein-A magnetic Sepharose beads (GE Healthcare) and 5ul Anti-Aiolos D1C1E (CST, Cat. Nr. 15103S) were used. Beads for each step were washed twice with TE and then blocked in 10% BSA.

For pre-clearing, beads were added to chromatin and incubated at 4C for 2h with rotation. After that, 1% was collected as input sample. anti-Aiolos was added to the pre-cleared chromatin and incubated o/n at 4C with rotation. The next day, an aliquot of blocked beads was added to the chromatin and incubated for 2h with rotation at 4C. Next, the beads were removed, and the supernatant was incubated again with beads as before. The beads were then combined and washed as follows for 10min at 4C with rotation: twice with RIPA [150mM NaCl, 50mM tris/HCl ph=8, 0.1% SDS, 1% Tergitol, 0.5% Na-deoxycholate], twice with high

salt buffer [500mM NaCl, 50mM Tris/HCl ph=8, 0.1% SDS, 1% Nonidet P-40], twice with LiCl buffer [250mM LiCl, 50mM Tris/HCl ph=8, 0.5% Na-deoxycholate, 1% Nonidet P-40], and twice with TE. Beads were then eluted in 75ul elution buffer [1% SDS, 100mM $NaHCO_3$ (fresh)] for 15min at RT with 600rpm shaking in a thermomixer. Supernatant was collected and beads were eluted again as before. Eluates were then pooled and crosslinks were reversed in [200mM NaCl, 10mM EDTA, 20mM Tris/HCl pH=6.5, 300ug/ml Proteinase K] by incubating o/n at 55C. Next, 300ul water were added containing RNaseA (100ug/ml final) and incubated for 30min at 37C. DNA was then purified using the ChIP DNA Clean & ConcentratorTM Kit (Zymo research D5205) according to the manufacturers protocol.

Library Preparation and Sequencing:

Library was prepared using the NEBNext Ultra II DNA Library kit according to the manufacturers protocol. 500pg-1ng DNA were used. Library was amplified for 7-11 cycles and cleanup was performed using AMPure XP beads (Beckman Coulter, Cat. Nr. A63881) Sequencing was performed in house by our core facility using HiSeqV4 SR50. Reads were mapped to mm10, peaks were called using MACS2 and peak to gene assignment.

4.11 mRNA-Seq

Spleens were harvested, stained and sorted as described above.

For sequencing in rescued MZ B cells, the following steps were performed: Total RNA extraction was performed using the RNeasy Plus Mini Kit (Qiagen, Cat. Nr. 74134) according to the manufacturers protocol. From 5-6ug total RNA, the mRNA was purified twice using the Dynabeads mRNA purification kit (ThermoFisher) according to the manufacturers protocol. Cleanup was performed again by using the RNeasy Plus mini Kit. All steps were monitored by analysis on a Fragment Analyzer. cDNA synthesis was performed using the SuperScript VILO cDNA Synthesis Kit (Invitrogen, Cat. Nr. 11754-050) according to the manufacturers protocol. The final cDNA was cleaned with MinElute reaction cleanup kit (Qiagen, Cat.Nr. 28204).

Library was prepared using the NEBNext Ultra II DNA Library kit according to the manufacturers protocol. 500pg-1ng DNA were used. Library was amplified for 9-13 cycles and cleanup was performed using AMPure XP beads (Beckman Coulter, Cat. Nr. A63881)

Sequencing in T1/T2 transitional B cells: Total RNA was prepared by using the NEB Monarch total RNA Miniprel Kit (NEB, Cat.Nr. T2010S) with the recommended on-column DNase treatment. Next, mRNA was purified with the NEBNext Poly(A) mRNA magnetic

isolation module (NEB, Cat. Nr. E7490). Finally, the library was prepared with the NEBNext Ultra II Directional RNA Library Prep Kit for Illumina (NEB, Cat.Nr. E7760S) with 9-11 cycles of amplification followed by two rounds of AMPure XP bead cleanup (Beckman Coulter, Cat. Nr. A63881).

Reads were quality trimmed and mapped to mm10 by our NGS sequencing facility. We then counted the number of reads per gene and performed pairwise RNA-Seq analysis using DESeq2 v1.2.10.

6 References:

1. Pieper, K.; Grimbacher, B.; Eibel, H. B-cell biology and development. Journal of Allergy and Clinical Immunology 2013, 131(4) 10.1016/j.jaci.2013.01.046.
2. Medvinsky, A.; Rybtsov, S.; Taoudi, S. Embryonic origin of the adult hematopoietic system: advances and questions. Development 2011, 138(6) 10.1242/dev.040998.
3. Schatz, D.G.; Ji, Y. Recombination centres and the orchestration of V(D)J recombination. Nature Reviews Immunology 2011, 11(4) 10.1038/nri2941.
4. Feeney, A.J. Epigenetic regulation of antigen receptor gene rearrangement. Current Opinion in Immunology 2011, 23(2) 10.1016/j.coi.2010.12.008.
5. Jhunjhunwala, S.; van Zelm, M.C.; Peak, M.M.; Cutchin, S.; Riblet, R.; van Dongen, J.J.M.; et al. The 3D Structure of the Immunoglobulin Heavy-Chain Locus: Implications for Long-Range Genomic Interactions. Cell 2008, 133(2) 10.1016/j.cell.2008.03.024.
6. Sun, A.; Novobrantseva, T.I.; Coffre, M.; Hewitt, S.L.; Jensen, K.; Skok, J.A.; et al. V_H replacement in primary immunoglobulin repertoire diversification. Proceedings of the National Academy of Sciences 2015, 112(5) 10.1073/pnas.1418001112.
7. Nemazee, D. Mechanisms of central tolerance for B cells. Nature Reviews Immunology 2017, 17(5) 10.1038/nri.2017.19.
8. Winkler, T.H.; Mårtensson, I.-L. The Role of the Pre-B Cell Receptor in B Cell Development, Repertoire Selection, and Tolerance. Frontiers in Immunology 2018, 9 10.3389/fimmu.2018.02423.
9. Collins, A.M.; Watson, C.T. Immunoglobulin Light Chain Gene Rearrangements, Receptor Editing and the Development of a Self-Tolerant Antibody Repertoire. Frontiers in Immunology 2018, 9 10.3389/fimmu.2018.02249.
10. Aoki-Ota, M.; Torkamani, A.; Ota, T.; Schork, N.; Nemazee, D. Skewed Primary Igκ Repertoire and V–J Joining in C57BL/6 Mice: Implications for Recombination Accessibility and Receptor Editing. The Journal of Immunology 2012, 188(5) 10.4049/jimmunol.1103484.
11. Martin, V.G.; Wu, Y.-C.B.; Townsend, C.L.; Lu, G.H.C.; O'Hare, J.S.; Mozeika, A.; et al. Transitional B Cells in Early Human B Cell Development – Time to Revisit the Paradigm?. Frontiers in Immunology 2016, 7 10.3389/fimmu.2016.00546.
12. Pillai, S.; Cariappa, A.; Moran, S.T. MARGINAL ZONE B CELLS. Annual Review of Immunology 2005, 23(1) 10.1146/annurev.immunol.23.021704.115728.
13. Allman, D.; Pillai, S. Peripheral B cell subsets. Current Opinion in Immunology 2008, 20(2) 10.1016/j.coi.2008.03.014.
14. Cerutti, A.; Cols, M.; Puga, I. Marginal zone B cells: virtues of innate-like antibody-producing lymphocytes. Nature Reviews Immunology 2013, 13(2) 10.1038/nri3383.
15. Cinamon, G.; Zachariah, M.A.; Lam, O.M.; Foss, F.W.; Cyster, J.G. Follicular shuttling of marginal zone B cells facilitates antigen transport. Nature Immunology 2008, 9(1) 10.1038/ni1542.
16. Arnon, T.I.; Horton, R.M.; Grigorova, I.L.; Cyster, J.G. Visualization of splenic marginal zone B-cell shuttling and follicular B-cell egress. Nature 2013, 493(7434) 10.1038/nature11738.
17. ZANDVOORT, A.; TIMENS, W. The dual function of the splenic marginal zone: essential for initiation of anti-TI-2 responses but also vital in the general first-line defense against blood-borne antigens. Clinical & Experimental Immunology 2002, 130(1) 10.1046/j.1365-2249.2002.01953.x.
18. Cinamon, G.; Matloubian, M.; Lesneski, M.J.; Xu, Y.; Low, C.; Lu, T.; et al. Sphingosine 1-phosphate receptor 1 promotes B cell localization in the splenic marginal zone. Nature Immunology 2004, 5(7) 10.1038/ni1083.

19. Tedford, K.; Steiner, M.; Koshutin, S.; Richter, K.; Tech, L.; Eggers, Y.; et al. The opposing forces of shear flow and sphingosine-1-phosphate control marginal zone B cell shuttling. Nature Communications 2017, 8(1) 10.1038/s41467-017-02482-4.
20. Ramos-Perez, W.D.; Fang, V.; Escalante-Alcalde, D.; Cammer, M.; Schwab, S.R. A map of the distribution of sphingosine 1-phosphate in the spleen. Nature Immunology 2015, 16(12) 10.1038/ni.3296.
21. Katakai, T.; Suto, H.; Sugai, M.; Gonda, H.; Togawa, A.; Suematsu, S.; et al. Organizer-Like Reticular Stromal Cell Layer Common to Adult Secondary Lymphoid Organs. The Journal of Immunology 2008, 181(9) 10.4049/jimmunol.181.9.6189.
22. Tsiantoulas, D.; Kiss, M.; Bartolini-Gritti, B.; Bergthaler, A.; Mallat, Z.; Jumaa, H.; et al. Secreted IgM deficiency leads to increased BCR signaling that results in abnormal splenic B cell development. Scientific Reports 2017, 7(1) 10.1038/s41598-017-03688-8.
23. Wen, L.; Brill-Dashoff, J.; Shinton, S.A.; Asano, M.; Hardy, R.R.; Hayakawa, K. Evidence of Marginal-Zone B Cell- Positive Selection in Spleen. Immunity 2005, 23(3) 10.1016/j.immuni.2005.08.007.
24. Horikawa, K.; Martin, S.W.; Pogue, S.L.; Silver, K.; Peng, K.; Takatsu, K.; et al. Enhancement and suppression of signaling by the conserved tail of IgG memory–type B cell antigen receptors. Journal of Experimental Medicine 2007, 204(4) 10.1084/jem.20061923.
25. Cariappa, A.; Takematsu, H.; Liu, H.; Diaz, S.; Haider, K.; Boboila, C.; et al. B cell antigen receptor signal strength and peripheral B cell development are regulated by a 9-O-acetyl sialic acid esterase. Journal of Experimental Medicine 2009, 206(1) 10.1084/jem.20081399.
26. Cariappa, A.; Tang, M.; Parng, C.; Nebelitskiy, E.; Carroll, M.; Georgopoulos, K.; et al. The Follicular versus Marginal Zone B Lymphocyte Cell Fate Decision Is Regulated by Aiolos, Btk, and CD21. Immunity 2001, 14(5) 10.1016/S1074-7613(01)00135-2.
27. Yam-Puc, J.C.; Zhang, L.; Zhang, Y.; Toellner, K.-M. Role of B-cell receptors for B-cell development and antigen-induced differentiation. F1000Research 2018, 7 10.12688/f1000research.13567.1.
28. Gerondakis, S.; Siebenlist, U. Roles of the NF- B Pathway in Lymphocyte Development and Function. Cold Spring Harbor Perspectives in Biology 2010, 2(5) 10.1101/cshperspect.a000182.
29. Tully, J.E.; Nolin, J.D.; Guala, A.S.; Hoffman, S.M.; Roberson, E.C.; Lahue, K.G.; et al. Cooperation between Classical and Alternative NF-κB Pathways Regulates Proinflammatory Responses in Epithelial Cells. American Journal of Respiratory Cell and Molecular Biology 2012, 47(4) 10.1165/rcmb.2012-0014OC.
30. Siebenlist, U.; Brown, K.; Claudio, E. Control of lymphocyte development by nuclear factor-κB. Nature Reviews Immunology 2005, 5(6) 10.1038/nri1629.
31. Guo, F.; Weih, D.; Meier, E.; Weih, F. Constitutive alternative NF-κB signaling promotes marginal zone B-cell development but disrupts the marginal sinus and induces HEV-like structures in the spleen. Blood 2007, 110(7) 10.1182/blood-2007-02-075143.
32. Jin, W.; Reiley, W.R.; Lee, A.J.; Wright, A.; Wu, X.; Zhang, M.; et al. Deubiquitinating Enzyme CYLD Regulates the Peripheral Development and Naive Phenotype Maintenance of B Cells. Journal of Biological Chemistry 2007, 282(21) 10.1074/jbc.M609952200.
33. Sun, S.-C. CYLD: a tumor suppressor deubiquitinase regulating NF-κB activation and diverse biological processes. Cell Death & Differentiation 2010, 17(1) 10.1038/cdd.2009.43.

34. Almaden, J. v.; Liu, Y.C.; Yang, E.; Otero, D.C.; Birnbaum, H.; Davis-Turak, J.; et al. B-cell survival and development controlled by the coordination of NF-κB family members RelB and cRel. Blood 2016, 127(10) 10.1182/blood-2014-10-606988.
35. Goudeau, B.; Huetz, F.; Samson, S.; di Santo, J.P.; Cumano, A.; Beg, A.; et al. I B /I B deficiency reveals that a critical NF- B dosage is required for lymphocyte survival. Proceedings of the National Academy of Sciences 2003, 100(26) 10.1073/pnas.2535880100.
36. Fabian, M.R.; Sonenberg, N. The mechanics of miRNA-mediated gene silencing: a look under the hood of miRISC. Nature Structural & Molecular Biology 2012, 19(6) 10.1038/nsmb.2296.
37. Boldin, M.P.; Taganov, K.D.; Rao, D.S.; Yang, L.; Zhao, J.L.; Kalwani, M.; et al. miR-146a is a significant brake on autoimmunity, myeloproliferation, and cancer in mice. Journal of Experimental Medicine 2011, 208(6) 10.1084/jem.20101823.
38. King, J.K.; Ung, N.M.; Paing, M.H.; Contreras, J.R.; Alberti, M.O.; Fernando, T.R.; et al. Regulation of Marginal Zone B-Cell Differentiation by MicroRNA-146a. Frontiers in Immunology 2017, 7 10.3389/fimmu.2016.00670.
39. Iwahashi, S.; Maekawa, Y.; Nishida, J.; Ishifune, C.; Kitamura, A.; Arimochi, H.; et al. Notch2 regulates the development of marginal zone B cells through Fos. Biochemical and Biophysical Research Communications 2012, 418(4) 10.1016/j.bbrc.2012.01.082.
40. Flores, A.N.; McDermott, N.; Meunier, A.; Marignol, L. NUMB inhibition of NOTCH signalling as a therapeutic target in prostate cancer. Nature Reviews Urology 2014, 11(9) 10.1038/nrurol.2014.195.
41. Moran, S.T.; Cariappa, A.; Liu, H.; Muir, B.; Sgroi, D.; Boboila, C.; et al. Synergism between NF-κB1/p50 and Notch2 during the Development of Marginal Zone B Lymphocytes. The Journal of Immunology 2007, 179(1) 10.4049/jimmunol.179.1.195.
42. Hozumi, K.; Negishi, N.; Suzuki, D.; Abe, N.; Sotomaru, Y.; Tamaoki, N.; et al. Delta-like 1 is necessary for the generation of marginal zone B cells but not T cells in vivo. Nature Immunology 2004, 5(6) 10.1038/ni1075.
43. Tan, J.B.; Xu, K.; Cretegny, K.; Visan, I.; Yuan, J.S.; Egan, S.E.; et al. Lunatic and Manic Fringe Cooperatively Enhance Marginal Zone B Cell Precursor Competition for Delta-like 1 in Splenic Endothelial Niches. Immunity 2009, 30(2) 10.1016/j.immuni.2008.12.016.
44. Hammad, H.; Vanderkerken, M.; Pouliot, P.; Deswarte, K.; Toussaint, W.; Vergote, K.; et al. Transitional B cells commit to marginal zone B cell fate by Taok3-mediated surface expression of ADAM10. Nature Immunology 2017, 18(3) 10.1038/ni.3657.
45. Tanigaki, K.; Han, H.; Yamamoto, N.; Tashiro, K.; Ikegawa, M.; Kuroda, K.; et al. Notch–RBP-J signaling is involved in cell fate determination of marginal zone B cells. Nature Immunology 2002, 3(5) 10.1038/ni793.
46. Simonetti, G.; Carette, A.; Silva, K.; Wang, H.; de Silva, N.S.; Heise, N.; et al. IRF4 controls the positioning of mature B cells in the lymphoid microenvironments by regulating NOTCH2 expression and activity. Journal of Experimental Medicine 2013, 210(13) 10.1084/jem.20131026.
47. Rebollo, A.; Schmitt, C. Ikaros, Aiolos and Helios: Transcription regulators and lymphoid malignancies. Immunology & Cell Biology 2003, 81(3) 10.1046/j.1440-1711.2003.01159.x.
48. Wang, J.-H.; Avitahl, N.; Cariappa, A.; Friedrich, C.; Ikeda, T.; Renold, A.; et al. Aiolos Regulates B Cell Activation and Maturation to Effector State. Immunity 1998, 9(4) 10.1016/S1074-7613(00)80637-8.
49. Fan, Y.; Lu, D. The Ikaros family of zinc-finger proteins. Acta Pharmaceutica Sinica B 2016, 6(6) https://doi.org/10.1016/j.apsb.2016.06.002.

50. Sharma, S.; Orlowski, G.; Song, W. Btk Regulates B Cell Receptor-Mediated Antigen Processing and Presentation by Controlling Actin Cytoskeleton Dynamics in B Cells. The Journal of Immunology 2009, 182(1) 10.4049/jimmunol.182.1.329.
51. Barrington, R.A.; Zhang, M.; Zhong, X.; Jonsson, H.; Holodick, N.; Cherukuri, A.; et al. CD21/CD19 Coreceptor Signaling Promotes B Cell Survival during Primary Immune Responses. The Journal of Immunology 2005, 175(5) 10.4049/jimmunol.175.5.2859.
52. You, Y.; Zhao, H.; Wang, Y.; Carter, R.H. Cutting Edge: Primary and Secondary Effects of CD19 Deficiency on Cells of the Marginal Zone. The Journal of Immunology 2009, 182(12) 10.4049/jimmunol.0804295.
53. Hippen, K.L.; Buhl, A.M.; D'Ambrosio, D.; Nakamura, K.; Persin, C.; Cambier, J.C. FcγRIIB1 Inhibition of BCR-Mediated Phosphoinositide Hydrolysis and Ca2+ Mobilization Is Integrated by CD19 Dephosphorylation. Immunity 1997, 7(1) 10.1016/S1074-7613(00)80509-9.
54. Vilagos, B.; Hoffmann, M.; Souabni, A.; Sun, Q.; Werner, B.; Medvedovic, J.; et al. Essential role of EBF1 in the generation and function of distinct mature B cell types. Journal of Experimental Medicine 2012, 209(4) 10.1084/jem.20112422.
55. Cortés, M.; Georgopoulos, K. Aiolos Is Required for the Generation of High Affinity Bone Marrow Plasma Cells Responsible for Long-Term Immunity. Journal of Experimental Medicine 2004, 199(2) 10.1084/jem.20031571.
56. Murtaugh, L.C.; Stanger, B.Z.; Kwan, K.M.; Melton, D.A. Notch signaling controls multiple steps of pancreatic differentiation. Proceedings of the National Academy of Sciences 2003, 100(25) 10.1073/pnas.2436557100.
57. Koo, C.Z.; Harrison, N.; Noy, P.J.; Szyroka, J.; Matthews, A.L.; Hsia, H.-E.; et al. The tetraspanin Tspan15 is an essential subunit of an ADAM10 scissor complex. Journal of Biological Chemistry 2020, 295(36) 10.1074/jbc.RA120.012601.
58. Jouannet, S.; Saint-Pol, J.; Fernandez, L.; Nguyen, V.; Charrin, S.; Boucheix, C.; et al. TspanC8 tetraspanins differentially regulate the cleavage of ADAM10 substrates, Notch activation and ADAM10 membrane compartmentalization. Cellular and Molecular Life Sciences 2016, 73(9) 10.1007/s00018-015-2111-z.
59. Matthews, A.L.; Szyroka, J.; Collier, R.; Noy, P.J.; Tomlinson, M.G. Scissor sisters: regulation of ADAM10 by the TspanC8 tetraspanins. Biochemical Society Transactions 2017, 45(3) 10.1042/BST20160290.
60. Zhang, Y.; Zhu, G.; Xiao, H.; Liu, X.; Han, G.; Chen, G.; et al. CD19 regulates ADAM28-mediated Notch2 cleavage to control the differentiation of marginal zone precursors to MZ B cells. Journal of Cellular and Molecular Medicine 2017, 21(12) 10.1111/jcmm.13276.
61. Suzuki, A.; Kaisho, T.; Ohishi, M.; Tsukio-Yamaguchi, M.; Tsubata, T.; Koni, P.A.; et al. Critical Roles of Pten in B Cell Homeostasis and Immunoglobulin Class Switch Recombination. Journal of Experimental Medicine 2003, 197(5) 10.1084/jem.20021101.
62. Lemieux, G.A.; Blumenkron, F.; Yeung, N.; Zhou, P.; Williams, J.; Grammer, A.C.; et al. The Low Affinity IgE Receptor (CD23) Is Cleaved by the Metalloproteinase ADAM10. Journal of Biological Chemistry 2007, 282(20) 10.1074/jbc.M608414200.
63. Liu, C.; Richard, K.; Wiggins, M.; Zhu, X.; Conrad, D.H.; Song, W. CD23 can negatively regulate B-cell receptor signaling. Scientific Reports 2016, 6(1) 10.1038/srep25629.
64. Rip, J.; de Bruijn, M.J.W.; Kaptein, A.; Hendriks, R.W.; Corneth, O.B.J. Phosphoflow Protocol for Signaling Studies in Human and Murine B Cell Subpopulations. The Journal of Immunology 2020, 204(10) 10.4049/jimmunol.1901117.

65. Yang, L.; Miao, L.; Liang, F.; Huang, H.; Teng, X.; Li, S.; et al. The mTORC1 effectors S6K1 and 4E-BP play different roles in CNS axon regeneration. Nature Communications 2014, 5(1) 10.1038/ncomms6416.
66. Biever, A.; Valjent, E.; Puighermanal, E. Ribosomal Protein S6 Phosphorylation in the Nervous System: From Regulation to Function. Frontiers in Molecular Neuroscience 2015, 8 10.3389/fnmol.2015.00075.
67. Meena, N.K.; Pattanayak, S.P.; Ben-Nun, Y.; Benhamron, S.; Kumar, S.; Merquiol, E.; et al. mTORC1 activation in B cells confers impairment of marginal zone microarchitecture by exaggerating cathepsin activity. Immunology 2018, 155(4) 10.1111/imm.12996.
68. Limon, J.J.; Fruman, D.A. Akt and mTOR in B Cell Activation and Differentiation. Frontiers in Immunology 2012, 3 10.3389/fimmu.2012.00228.
69. Dibble, C.C.; Asara, J.M.; Manning, B.D. Characterization of Rictor Phosphorylation Sites Reveals Direct Regulation of mTOR Complex 2 by S6K1. Molecular and Cellular Biology 2009, 29(21) 10.1128/MCB.00735-09.
70. Janas, M.L.; Hodson, D.; Stamataki, Z.; Hill, S.; Welch, K.; Gambardella, L.; et al. The Effect of Deleting p110δ on the Phenotype and Function of PTEN-Deficient B Cells. The Journal of Immunology 2008, 180(2) 10.4049/jimmunol.180.2.739.
71. Zhang, X.; Tang, N.; Hadden, T.J.; Rishi, A.K. Akt, FoxO and regulation of apoptosis. Biochimica et Biophysica Acta (BBA) - Molecular Cell Research 2011, 1813(11) 10.1016/j.bbamcr.2011.03.010.